

## Two-dimensional quantum Heisenberg antiferromagnet at low temperatures

Sudip Chakravarty\*

*Department of Physics, State University of New York at Stony Brook, Stony Brook, New York 11794*

Bertrand I. Halperin and David R. Nelson

*Lyman Laboratory of Physics, Harvard University, Cambridge, Massachusetts 02138*

(Received 18 August 1988)

It is argued that the long-wavelength, low-temperature behavior of a two-dimensional quantum Heisenberg antiferromagnet can be described by a quantum nonlinear  $\sigma$  model in two space plus one time dimension, at least in the range of parameters where the model has long-range order at zero temperature. The properties of the quantum nonlinear  $\sigma$  model are analyzed approximately using the one-loop renormalization-group method. When the model has long-range order at  $T=0$ , the long-wavelength behavior at finite temperatures can be described by a purely classical model, with parameters renormalized by the quantum fluctuations. The low-temperature behavior of the correlation length and the static and dynamic staggered-spin-correlation functions for the quantum antiferromagnet can be predicted, in principle, with no adjustable parameters, from the results of simulations of the classical model on a lattice, combined with a two-loop renormalization-group analysis of the classical nonlinear  $\sigma$  model, a calculation of the *zero-temperature* spin-wave stiffness constant and uniform susceptibility of the quantum antiferromagnet, and a one-loop analysis of the conversion from a lattice cutoff to the wave-vector cutoff introduced by quantum mechanics when the spin-wave frequency exceeds  $T/\hbar$ . Applying this approach to the spin- $\frac{1}{2}$  Heisenberg model on a square lattice, with nearest-neighbor interactions only, we obtain a result for the correlation length which is in good agreement with the data of Endoh *et al.* on  $\text{La}_2\text{CuO}_4$ , if the spin-wave velocity is assumed to be  $0.67 \text{ eV } \text{\AA}/\hbar$ . We also argue that the data on  $\text{La}_2\text{CuO}_4$  cannot be easily explained by any model in which an isolated  $\text{CuO}_2$  layer would not have long-range antiferromagnetic order at  $T=0$ . Our theory also predicts a quasielastic peak of a few meV width at 300 K when  $k\xi \ll 1$  (where  $k$  is wave-vector transfer and  $\xi$  is the correlation length). The extent to which this dynamical prediction agrees with experiments remains to be seen. In an appendix, we discuss the effect of introducing a frustrating second-nearest-neighbor coupling for the antiferromagnet on the square lattice.

### I. INTRODUCTION

The discovery of high-temperature superconductors has led to renewed efforts, both theoretical and experimental, to understand quantum antiferromagnets. Much of this interest stems from Anderson's original suggestion<sup>1</sup> that novel quantum-spin fluctuations in  $\text{CuO}_2$  layers may be responsible for superconductivity in doped materials such as  $\text{La}_{2-x}\text{Sr}_x\text{CuO}_4$  and  $\text{YBa}_2\text{Cu}_3\text{O}_{6+x}$ . Since then a number of possible mechanisms have been suggested<sup>2</sup> in which the quantum nature of the Cu spins plays an important role in producing high-temperature superconductivity. The aim of the present investigation, however, is to obtain a better understanding of the stoichiometric insulating quantum antiferromagnet, in light of recent neutron scattering measurements<sup>3,4</sup> in  $\text{La}_2\text{CuO}_4$ . Although the subject of quantum antiferromagnets is rather old, there are a number of unresolved issues which are particularly pressing in the present context. Some of the results reported here were briefly presented in a recent letter.<sup>5</sup>

Our analysis of the experiments leads us to believe that the undoped  $\text{La}_2\text{CuO}_4$  can be modeled rather well by a nearest-neighbor  $S = \frac{1}{2}$  antiferromagnetic (AF) Heisenberg Hamiltonian on a square lattice with a large exchange constant  $J$  of order 1200 K; in particular, the

interplanar coupling and the spin anisotropies are both very small. The present estimate<sup>6</sup> for the interplanar coupling  $J'$  is  $10^{-5}J$ . Such a small  $J'$  has very little effect on the two-dimensional spin fluctuations seen above the three-dimensional Néel temperature  $T_N$ ; the critical region in which  $J'$  is expected to have a major effect is extremely narrow. One can also show that such a small  $J'$  has very little effect on the *zero-temperature* properties calculated assuming that the system consists of isolated  $\text{CuO}_2$  layers (see Appendix F). However, the interplanar coupling is believed responsible for the fact that there is long-range order at finite temperatures, below  $T_N$ , as even a tiny interplanar coupling can induce long-range order when the in-plane correlation length becomes sufficiently large.

In principle, weak Ising-like anisotropies can lead to qualitative changes from Heisenberg behavior for an isolated layer. However, experimental estimates of the spin anisotropy in  $\text{La}_2\text{CuO}_4$  suggest that this anisotropy is less important than the interlayer coupling in this system.<sup>7</sup>

In the present paper, we shall focus attention on the pure two-dimensional (2D) Heisenberg model and the properties of  $\text{La}_2\text{CuO}_4$  that can be understood using it. We assume that the dominant interaction in  $\text{La}_2\text{CuO}_4$  is the nearest-neighbor antiferromagnetic exchange, though

we shall also investigate a model with frustrating second-neighbor exchange.

For many years it has been generally believed that the 2D  $S = \frac{1}{2}$  AF (two-dimensional nearest-neighbor  $S = \frac{1}{2}$  Heisenberg antiferromagnet on a square lattice) has long-range order (LRO) at  $T=0$ . In an important paper Anderson<sup>8</sup> argued that even though the staggered magnetization may be reduced, the Néel state is stable against quantum fluctuations at  $T=0$ . A number of recent numerical calculations<sup>9</sup> support this view quite strongly. Since none of these studies are rigorous, they can be challenged, however. Indeed, Anderson himself speculated in a later paper that long-range order could be destroyed by quantum fluctuations.<sup>10</sup>

There are rigorous results due to Neves and Peres<sup>11</sup> based on an extension of the work due to Dyson, Lieb, and Simon,<sup>12</sup> which show that at  $T=0$  there is LRO for  $S \geq \frac{3}{2}$ ; after correction of a minor error in Ref. 11, it has proved possible to extend<sup>13</sup> these results to the case of  $S=1$ . An extension of the proof to  $S = \frac{1}{2}$  has not yet been achieved, however.

Until recently, accurate experimental realizations of the theoretical model were not known. In this respect recent neutron measurements in  $\text{La}_2\text{CuO}_4$  have significantly changed the situation. However, to compare with experiments, it is necessary that we are able to deduce the properties of the 2D  $S = \frac{1}{2}$  AF at finite temperatures. It is particularly important to use a finite-temperature analysis in view of the Hohenberg-Mermin-Wagner theorem<sup>14</sup> which shows rigorously that there cannot be long-range order in a two-dimensional Heisenberg system at  $T \neq 0$ .

It is illuminating to consider the issues addressed in this paper in the context of a  $1/S$  expansion<sup>8,15-17</sup> for the quantum spin- $\frac{1}{2}$  antiferromagnet on a square lattice with Hamiltonian

$$\mathcal{H} = J \sum_{\langle i,j \rangle} \mathbf{S}_i \cdot \mathbf{S}_j + J'' \sum_{\langle\langle k,l \rangle\rangle} \mathbf{S}_i \cdot \mathbf{S}_j, \quad (1.1)$$

where  $J > 0$  and  $J'' > 0$  represent nearest-neighbor and next-nearest-neighbor couplings, respectively. We may define the staggered magnetization  $N$  such that in an ordered ground state

$$\langle \mathbf{S}_i \rangle = \pm N \hat{\mathbf{n}}_0, \quad (1.2)$$

where  $\hat{\mathbf{n}}_0$  is an arbitrary unit vector, independent of the site, and the sign  $\pm$  is opposite on the two sublattices. When  $S \rightarrow \infty$ , the spins behave like classical vectors and the ground state is the fully aligned Néel state with  $N=S$ . The next-nearest-neighbor coupling  $J''$  opposes the local Néel order, although it does not change the classical ground state for small  $J''/J$ . For finite  $S$ , quantum-mechanical fluctuations reduce the staggered magnetization in the ground state, even if  $J''=0$ .

In Appendix A we calculate the reduction in the classical staggered magnetization to second order in  $1/S$ :

$$N = S \left[ 1 - \alpha(J''/J)S^{-1} + (J''/J)I_1(J''/J) \right. \\ \left. \times I_2(J''/J)S^{-2} + O(S^{-3}) \right]. \quad (1.3)$$

The positive functions  $\alpha(J''/J)$ ,  $I_1(J''/J)$ , and  $I_2(J''/J)$  are tabulated in Appendix A. As shown in Fig. 1, the fall-off in the staggered magnetization with decreasing  $S$  becomes more pronounced for nonzero  $J''/J$ . Although it is hard to draw precise conclusions from an alternating series such as (1.3), it is plausible that there exists a critical value of the spin  $S = S_c(J''/J)$  below which the staggered magnetization vanishes. There is growing evidence that  $S_c$  is less than the lowest physically accessible value  $S = \frac{1}{2}$  for  $J''=0$ .<sup>9</sup> It may be possible, however, to choose  $J''$  large enough so that  $S_c > \frac{1}{2}$ , in which case a number of interesting ideas about "quantum disordered" antiferromagnets could be tested for  $S = \frac{1}{2}$ . As stated above, however, our analysis of the neutron scattering experiments<sup>3,4</sup> strongly suggests that this is *not* the case for defect-free  $\text{La}_2\text{CuO}_4$ .

Note that if the third term in Eq. (1.3) were ignored, one would conclude that  $N$  vanishes at  $(J''/J)=0.38$  for  $S = \frac{1}{2}$ . The presence of the third term, however, invalidates such a conclusion.<sup>18</sup>

The principal purposes of the present paper are (a) to predict the static and the dynamic properties of the  $S = \frac{1}{2}$  AF at low temperatures assuming that there is long-range order at  $T=0$ , and (b) to compare our theoretical work with experiments on  $\text{La}_2\text{CuO}_4$ .

We begin by constructing an effective continuum field theory described by a model which is a quantum-mechanical generalization of the classical nonlinear  $\sigma$  model.<sup>19</sup> The classical model is known to capture correctly the long-wavelength physics contained in the classical Heisenberg lattice models where the spins are represented by three-component unit vectors. As we shall argue later, we expect the quantum-mechanical nonlinear  $\sigma$  model<sup>5</sup> (QNL $\sigma$ M) to do the same as far as the low-energy, long-wavelength behavior of the corresponding quantum model is concerned. In addition to  $d$  spatial dimensions, one needs an extra dimension, the imaginary time dimension,

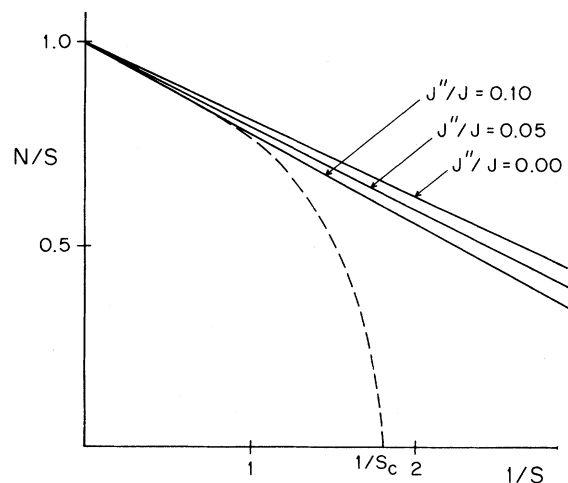


FIG. 1. Staggered magnetization  $N$  as a function of  $1/S$ , within spin-wave approximation, for different values of the ratios of next-nearest-neighbor to nearest-neighbor couplings  $J''/J$ . The dashed curve is a plausible guess as to how the system may disorder, for a larger value of  $J''/J$ .

to specify the QNL $\sigma$ M. The presence of the imaginary time dimension is a reflection of the quantum fluctuations. Thus we shall often refer to this model as a  $(d+1)$ -dimensional model. The thickness in the imaginary time direction is inversely proportional to the temperature, and hence goes to infinity as the temperature goes to zero. At  $T=0$ , the model is described by a dimensionless coupling constant which plays the role of  $1/S$  in Fig. 1.

Alternately, it is possible to describe the same system using a "soft-spin" three-component  $\phi^4$  quantum field theory in  $d$  spatial and 1 imaginary time dimension where the  $\phi$  field has  $O(3)$  symmetry. However, the fixed length QNL $\sigma$ M is more convenient in  $d=2$  at finite temperatures. For  $d=2$ , and at  $T=0$ , the system is described by  $(2+1)$  or a "three-dimensional" field theory. In this case, a  $\phi^4$  theory may have certain advantages over the QNL $\sigma$ M. Although we shall mainly use the QNL $\sigma$ M, occasionally we shall use some well-known results from the  $\phi^4$  theory.

QNL $\sigma$ M has two independent dimensional parameters: the local spin stiffness constant  $\rho_s^0$ , and the local uniform magnetic susceptibility  $\chi_\perp^0$ , in the direction perpendicular to the local staggered magnetization. For the microscopic model (1.1) with  $J''=0$  and lattice constant  $a$ , these parameters are just  $\rho_s^0 = JS^2 a^{2-d}$  and  $\chi_\perp^0 = \hbar^2/4d Ja^d$  in the limit  $S \rightarrow \infty$ . These parameters are defined on a short-wavelength microscopic scale. We shall see later that within our scheme it is possible to fix  $\rho_s^0$  and  $\chi_\perp^0$  for arbitrary  $S$  if we know the corresponding observable macroscopic parameters which are the long-wavelength properties of the system at  $T=0$ . Instead of working with  $\rho_s^0$  and  $\chi_\perp^0$  it is also possible to work with a dimensionless parameter  $\bar{g}_0$  and one dimensional parameter, such as the spin-wave velocity  $c$ .

Given the effective-field theory described by the QNL $\sigma$ M, it is straightforward to derive one-loop renormalization-group equations to analyze the model. We combine the methods developed by Hertz<sup>20</sup> and Young<sup>21</sup> for related quantum spin models with the momentum shell recursion techniques developed by Nelson and Pelcovits<sup>22</sup> for the classical version of the same model. The renormalization group leads directly to the correlation length as a function of temperature. Although the system is disordered at any  $T \neq 0$ , one can identify three separate regions in the parameter space on the basis of the behavior of the correlation length as a function of temperature. In the region of greatest experimental interest, which we designate as the renormalized classical regime, one can do better than a one-loop calculation of the correlation length. It is possible to exploit the available computer simulations for the classical lattice rotator model (CLRM) and the two-loop renormalization-group equations to compute the correlation length for our problem. The resulting expression for the correlation length contains *no* adjustable parameters. In this renormalized classical regime, comparison with the CLRM yields also a number of other useful results pertaining to the dynamics of the system.

Aside from the principal purposes described above we have a secondary purpose. We would also like to explore the low-temperature behavior of the QNL $\sigma$ M in the re-

gimes for which the  $T=0$  state has no LRO. As was mentioned earlier, such regimes might be achieved by introducing frustrating next-nearest-neighbor interactions, or by introducing several spins per unit cell. This analysis can also be carried out with the help of the renormalization-group equations.

In the quantum disordered phase of the nonlinear  $\sigma$  model, at  $T=0$ , one finds that the elementary excitations are bosons, with a gap in the energy spectrum. The gap vanishes only at the critical value of the coupling constant where the transition to Néel order occurs.

Several comments are in order. The first concerns the validity of the QNL $\sigma$ M approach. QNL $\sigma$ M is the simplest continuum model with the correct spin-wave spectrum at long wavelengths. However, for the theory to be nontrivial it must also include correctly the interaction between spin waves. We shall argue later that the interactions between spin waves at long wavelengths are entirely determined by the symmetries of the model, and are therefore correctly described by the QNL $\sigma$ M. A microscopic derivation, starting from the lattice Heisenberg model, of the QNL $\sigma$ M in the  $S \rightarrow \infty$  (semiclassical) limit was first given by Haldane,<sup>23</sup> and later by Affleck.<sup>24</sup> As was recognized by these authors, it is difficult to continue this mapping to smaller values of  $S$ : Even if the form of the Lagrangian is correct, it is difficult to obtain sufficiently accurate values for the parameters of the model from large- $S$  considerations. Moreover, these parameters depend sensitively on the precise manner in which the continuum limit is taken. As explained earlier, we circumvent this difficulty by considering the coupling constants as phenomenological input parameters to be determined from experiments. Thus, it seems reasonable to assert that the long-wavelength, low-energy physics of the QNL $\sigma$ M are identical to those of the lattice quantum Heisenberg model.

There is one remaining point that deserves more careful attention. Our QNL $\sigma$ M does not distinguish between integer and half-integer spins. It has been argued<sup>25</sup> that one may need, in addition, certain topological terms in order to distinguish between integer and half-integer spins. For the  $(1+1)$ -dimensional model this almost certainly seems to be the case as was first pointed out by Haldane.<sup>26</sup> In fact, the "Haldane conjecture" that the excitation spectrum is gapless for spin chains with half integer spins, but the spectrum should have an energy gap for integer spins, appears to have received considerable numerical support.<sup>27</sup>

The situation may be quite different for  $(2+1)$ -dimensional models. Based on an extension of a theorem due to Lieb, Schultz, and Mattis<sup>28</sup> valid for an  $S = \frac{1}{2}$  antiferromagnetic periodic chain of length  $L$ , Affleck<sup>29</sup> has argued that integer and half-integer spin systems may behave differently even in two dimensions. Also, on the basis of the local  $SU(2)$  symmetry of the Heisenberg model, Zou<sup>30</sup> claims to have shown that the spin- $\frac{1}{2}$  system, in the continuum limit, reduces to a problem of massless fermions coupled to  $SU(2)$  gauge field in  $(2+1)$  dimensions. Recently, Dzyaloshinskii, Polyakov, and Wiegmann<sup>31</sup> have conjectured that a  $(2+1)$ -dimensional field theory that correctly represents spin- $S$  antiferromagnets

must contain in addition to our QNL $\sigma$ M a Hopf term,<sup>32</sup> i.e., the action must contain an additional term  $\hbar\theta H^{\text{Hopf}}$ , where  $\theta=2\pi S(\text{mod}2\pi)$ . Such a term, if present, can in principle distinguish between integer and half-integer spins; the situation would be analogous to the topological  $\theta$  term in the corresponding (1+1)-dimensional model. Subsequently, careful analysis of the spin- $S$  Heisenberg antiferromagnet on a two-dimensional square lattice has led a number of authors<sup>33</sup> to conclude that to the extent that the unit vector field  $\hat{\Omega}(x,y,t)$  characterizing the continuum field theory is well defined (continuous) at all points *no such Hopf term exists*. Tentatively, one might therefore conclude that our QNL $\sigma$ M does correctly represent the continuum limit of the two-dimensional spin- $S$  Heisenberg antiferromagnet on a square lattice. However, Haldane<sup>34</sup> has argued that once the assumption that  $\hat{\Omega}(x,y,t)$  is everywhere well defined is relaxed, it is possible that an intrinsic dependence on the quantized value of  $S$  will appear through the creation of hedgehog singularities. Haldane's analysis suggests a difference between even and odd integer spins as well as between integer and half integer, and the QNL $\sigma$ M gives a correct description of the quantum disordered phase at  $T=0$  only for the case of even integer spin. (This conclusion is also supported by a recent analysis by Read and Sachdev.<sup>35</sup>) Nevertheless, *it seems very unlikely that taking these additional topological effects into account would change our conclusions for the low-temperature behavior in the parameter region where there is Néel order at  $T=0$* . In the ordered phase the topological defects are massive, and, hence, cannot contribute significantly at low energies and at long wavelengths.

We have remarked earlier that there is much that one can learn from  $d=2$  classical models. We would like to further elaborate on this point. We shall see that for  $\bar{g}_0 < 1$ , the  $T=0$  state has LRO. In this regime there exists a length  $\xi_J$  (the Josephson correlation length)<sup>36</sup> which tends to infinity as  $\bar{g}_0 \rightarrow 1$ . Physically,  $\xi_J$  is a crossover length which separates, at  $T=0$ , the long-wavelength antiferromagnetic magnons from the shorter-wavelength critical fluctuations important near  $\bar{g}_0=1$ . However, for the values of  $\bar{g}_0$  of greatest experimental interest  $\xi_J$  turns out to be of the order of a few lattice spacings. We expect that quantum critical fluctuations will be unimportant for wave vectors  $k$  such that  $k < \xi_J^{-1}$ . It turns out, moreover, that the system will behave like a two-dimensional classical spin system whenever the additional inequality  $k < k_B T/\hbar c$  is obeyed. Both inequalities are satisfied in the experimentally relevant temperature range in Ref. 5.

We end our introduction by summarizing our most important results. In the regime in which the  $T=0$  state has LRO we find that as  $T \rightarrow 0$ , the correlation length  $\xi$  is given by

$$\xi = C_\xi a e^{2\pi\rho_s/k_B T}. \quad (1.4)$$

Here,  $a$  is the lattice spacing and  $\rho_s$  is the actual spin stiffness constant at  $T=0$ , i.e., with the quantum fluctuations taken into account. A two-loop *classical* correction to the exponential temperature dependence, proportional to  $T$ , combines with a *quantum-mechanical* correction factor, proportional to  $T^{-1}$ , to give the temperature-

independent overall prefactor of Eq. (1.4). The constant  $C_\xi$  is a "nonuniversal" *number* in the sense that it depends on the choice of the system. For example, we expect  $C_\xi$  for the nearest-neighbor 2D  $S=\frac{1}{2}$  AF to be different from a model which contains, in addition, next-nearest-neighbor interactions. However, once the model is specified,  $C_\xi$  can be uniquely determined from a microscopic calculation of the *zero-temperature* properties of the system. For the 2D  $S=\frac{1}{2}$  AF we calculate using classical numerical simulations and  $T=0$  spin-wave theory that  $C_\xi \approx 0.5$ . We find that the correlation lengths determined experimentally for  $\text{La}_2\text{CuO}_4$  can be well fit by the above formula with  $2\pi\rho_s=1175$  K and  $C_\xi=1$ . (The uncertainty in  $C_\xi$  is much larger than the uncertainty in  $\rho_s$ .) Since the experiments are not necessarily in the asymptotic low-temperature regime where (1.4) is supposed to be accurate, and since there are also uncertainties in the theoretical value, we consider the agreement (see Sec. VI) to be very satisfactory.

For the 2D  $S=\frac{1}{2}$  AF we can write

$$2\pi\rho_s = C_{\rho_s}(\hbar c/a), \quad (1.5)$$

where  $c$  is the spin-wave velocity at  $T=0$ , and  $C_{\rho_s}$  is estimated to be 0.576 from spin-wave theory. Thus the fitted value of  $\rho_s$  implies  $\hbar c=0.66$  eV Å. This value of  $\hbar c$  is quite consistent with the light scattering experiments of Lyons *et al.*,<sup>37</sup> who obtain  $\hbar c=0.74$  eV Å. It is also consistent with the recent<sup>38</sup> lower bound on  $\hbar c$  given by the neutron scattering experiments which is  $\hbar c > 0.6$  eV Å.

Our other important results include the predictions for the static and the dynamic structure factors. The results for the dynamic structure factor are derived within the context of the dynamic scaling hypothesis.<sup>39</sup> We shall use  $S(k)$  and  $S(k,\omega)$  to denote the static and dynamic structure factor for the order parameter of the nonlinear  $\sigma$  model or the staggered magnetization of the quantum antiferromagnet, so that  $k=0$  refers to the magnetic structure factor at the position of the antiferromagnetic Bragg peak. Then in the parameter regime where the QNL $\sigma$ M has Néel order at  $T=0$  we find

$$S(k=0) \propto T^2 \xi^2, \quad (1.6)$$

while the characteristic frequency scale  $\bar{\omega}_0$  which determines the dynamic structure factor is given by

$$\bar{\omega}_0 = \text{const} \left[ \frac{k_B T}{2\pi\rho_s} \right]^{1/2} \xi^{-1} c. \quad (1.7)$$

We believe that it should be possible to test our predictions for the dynamics as the experiments are made more precise.

Finally, we would like to emphasize that if we *assume* that  $\bar{g}_0 \geq 1$ , so that an isolated layer does not have LRO at  $T=0$ , then it would be necessary to choose an exceptionally large value of the interplanar coupling  $J'$ , comparable to  $J$ , in order to account for the actual observed ( $\sim 0.5\mu_B$ ) staggered magnetization as  $T \rightarrow 0$  in  $\text{La}_2\text{CuO}_4$ . For  $\bar{g}_0=1$ , scaling predicts that the staggered magnetization  $M$  at  $T=0$  due to interplanar coupling is

given by

$$M \propto \left( \frac{J'}{J} \right)^{(1+\eta_3)/(4-2\eta_3)}, \quad (1.8)$$

where  $\eta_3$  is the correlation function exponent for the 3D Heisenberg model and is approximately 0. A still smaller value of  $M$  is obtained, for a given value of  $J'$ , if we assume  $\bar{g}_0 > 1$ . A large value of  $J'$  is inconsistent with the fact that the observed spin correlations are two dimensional for  $T > T_N$ . Similar inconsistencies arise if one assumes large Ising-like spin anisotropies to account for the observed staggered magnetization. We believe that it is quite likely that *any* alternate description of the quantum disordered phase will run into the same difficulties in explaining the observed staggered magnetization as we find with the QNL $\sigma$ M for  $\bar{g}_0 \geq 1$ .

Our conclusions are similar to those obtained in several recent papers.<sup>40</sup> Arovas and Auerbach have introduced the Schwinger boson mean-field theory as a useful way to treat a large class of low-dimensional quantum Heisenberg models. They find the same exponential temperature dependence for the static correlation length [Eq. (1.7)], but their expression for the characteristic frequency  $\bar{\omega}_0$  controlling the dynamics differs from ours [Eq. (4.17)] by a factor of the square root of temperature. Grepel has applied mode coupling theory to the dynamics, using the static properties as input.<sup>40</sup> His results for the characteristic order-parameter frequency  $\bar{\omega}_0$  as well as for the spin-diffusion constant agree with ours.

## II. QUANTUM NONLINEAR $\sigma$ MODELS

### A. Definitions

The effective Euclidean action of the quantum-mechanical nonlinear  $\sigma$  model may be written in the form<sup>23</sup>

$$S_{\text{eff}}/\hbar = \frac{\rho_s^0}{2\hbar} \int_0^{\beta\hbar} d\tau \int d^d x \left[ |\nabla \hat{\mathbf{n}}|^2 + \frac{1}{c_0^2} \left| \frac{\partial \hat{\mathbf{n}}}{\partial \tau} \right|^2 \right], \quad (2.1)$$

where  $\hat{\mathbf{n}}$  is a three-component vector field which we interpret as the local staggered magnetization. The constraint  $|\hat{\mathbf{n}}| = 1$  is understood. There is a short-distance cutoff  $\Lambda^{-1}$  for the spatial integrals, but no such intrinsic cutoff exists for the imaginary time variable  $\tau$ . The fact that quantum fluctuations exist on all (imaginary) time scales is an intrinsic part of Feynman path integrals<sup>41</sup> that we would like to preserve. Here  $\rho_s^0$  is the bare spin-stiffness constant which is defined on the scale  $\Lambda^{-1}$ , and  $c_0$  is the bare spin-wave velocity at the same length scale. Because we employ a cutoff procedure which is not Lorentz invariant, the actual spin-wave velocity  $c$  which enters the spectrum of long-wavelength excitations at  $T=0$  may differ from  $c_0$  by a finite factor. By contrast, in a Lorentz invariant model, one has  $c = c_0$  precisely. This equality also holds in the present model if the calculations are restricted to one loop accuracy. The combination  $\rho_s^0 c_0^{-2} \equiv \chi_{\perp}^0$  may be identified as the local uniform magnetic susceptibility,

in the direction perpendicular to the local staggered magnetization (in units where  $g\mu_B/\hbar = 1$ ).<sup>42</sup> The partition function  $Z$  for this model is then given by [with  $\mathbf{n}(\beta\hbar) = \mathbf{n}(0)$ ]

$$Z \propto \int \mathcal{D}\mathbf{n}(\mathbf{x}, \tau) \delta(|\mathbf{n}| - 1) e^{-S_{\text{eff}}/\hbar}. \quad (2.2)$$

Instead of determining  $\rho_s^0$  and  $c_0$  from the large  $S$  limit<sup>25</sup> [where  $\rho_s^0 = JS^2 a^{2-d}$  and  $c_0 = 2\sqrt{d}JSa/\hbar$  for Eq. (1.1) with  $J''=0$ ] we take them as phenomenological input parameters. Later we shall show how to determine these parameters from the experimentally observed macroscopic parameters.

It is instructive to note how the classical limit of this model is approached at high temperatures. Let us first rewrite Eq. (2.1) in a dimensionless form by defining  $y = \Lambda x$  and  $u = \Lambda c_0 \tau$ . Then we can write

$$S_{\text{eff}}/\hbar = \frac{1}{2g_0} \int_0^{\beta\hbar c_0 \Lambda} du \int d^d y \left[ |\nabla \hat{\mathbf{n}}|^2 + \left| \frac{\partial \hat{\mathbf{n}}}{\partial u} \right|^2 \right], \quad (2.3)$$

where the dimensionless coupling constant  $g_0$  is given by

$$g_0 = \frac{\hbar c_0 \Lambda^{d-1}}{\rho_s^0}. \quad (2.4)$$

Now, when  $\beta\hbar c_0 \Lambda \ll 1$ , the configurations that dominate the partition function are such that  $\hat{\mathbf{n}}(x, \tau)$  is independent of  $\tau$ . Otherwise, the term  $|\partial \hat{\mathbf{n}}/\partial u|^2$  would be too large. In this limit we get

$$S_{\text{eff}}/\hbar \xrightarrow{\beta\hbar c_0 \Lambda \rightarrow 0} \frac{\rho_s^0 \Lambda^{2-d}}{2k_B T} \int d^d y |\nabla \hat{\mathbf{n}}|^2, \quad (2.5)$$

which is precisely the "action" for the extensively studied classical nonlinear  $\sigma$  model.<sup>19</sup> When  $\beta\hbar c_0 \Lambda$  is not very small compared to unity, however, the assumption that  $\hat{\mathbf{n}}$  is independent of  $\tau$  is no longer valid. The dependence of  $\hat{\mathbf{n}}$  on  $\tau$  then reflects the quantum fluctuations of the system.

It is clear from Eq. (2.3) that the action is *formally* equivalent to a classical  $(d+1)$ -dimensional nonlinear  $\sigma$  model in which one of the dimensions is finite. As  $T \rightarrow 0$ , the thickness in the imaginary time direction goes to infinity. It is important to note here the distinction between Heisenberg ferromagnets and antiferromagnets. Classically, ferromagnets and antiferromagnets have identical thermodynamic properties. This is no longer true for quantum statistical mechanics because one cannot separate statics from the dynamics of the system in this case. Since ferromagnets and antiferromagnets differ with respect to their dynamical properties, their thermodynamic properties calculated according to quantum statistical mechanics would also be very different. We shall see later that Eq. (2.3) embodies the dynamics of a Heisenberg antiferromagnet rather than a ferromagnet. On the other hand, in the classical limit where Eq. (2.5) applies, the model is equally applicable to ferromagnets or antiferromagnets.

The action given in Eq. (2.1) was first derived by Haldane in the large- $S$  limit, starting from the microscopic nearest-neighbor antiferromagnetic Heisenberg model for the  $(1+1)$ -dimensional case.<sup>25</sup> It was also remarked by

him that the derivation of an equivalence between the low-energy dynamics of the large-spin Heisenberg antiferromagnet and the  $O(3)$  nonlinear  $\sigma$  model is independent of dimension. Indeed, he gave the definition of the coupling constant  $g_0$  to be ( $S \rightarrow \infty$ )

$$g_0^H = \frac{2\sqrt{d}}{S}. \quad (2.6)$$

Haldane also suggested that for smaller values of  $S$  it may be more accurate to replace  $S$  by  $\sqrt{S(S+1)}$  in the above formula. It is also possible to motivate this model by a direct perturbation theory. Although we have no general proof, one can check, in the first few orders in perturbation theory, that the two models are identical in so far as the low-energy, long-wavelength properties are concerned. The perturbation theory on the quantum spin- $S$  antiferromagnetic Heisenberg model can be conveniently carried out by using Holstein-Primakoff transformation.<sup>43</sup>

### B. Quantum lattice rotator model

Our justification of the QNL $\sigma$ M will proceed by examining the long-wavelength, low-frequency properties predicted by a hydrodynamic analysis of the quantum nonlinear  $\sigma$  model, and comparing these with the hydrodynamics of the Heisenberg antiferromagnets. We shall see that for all regimes where the long-wavelength properties of the Heisenberg antiferromagnet have been previously studied, the dynamic properties are the same as for quantum nonlinear  $\sigma$  model, with the exception of the special case of half-integer spins in one dimension at  $T=0$ . This gives some support to our use of the QNL $\sigma$ M in the region of true interest to us, where results for the Heisenberg antiferromagnet have not been previously available—viz. the regime of low but finite temperatures at  $d=2$ .

In order to make the model precise, and to make contact more easily with ideas familiar in condensed-matter physics, we shall employ a lattice regularization for the  $d$ -space dimensions of the model. Then we may rewrite Eq. (2.1) as

$$\hbar^{-1} S_{\text{eff}} = \frac{b^d \rho_s^0}{2\hbar} \int_0^{\beta\hbar} d\tau \left[ \sum_i \left| \frac{d\hat{\mathbf{n}}_i}{c_0 d\tau} \right|^2 + \sum_{\langle i,j \rangle} \frac{|\hat{\mathbf{n}}_i - \hat{\mathbf{n}}_j|^2}{b^2} \right], \quad (2.7)$$

where  $\hat{\mathbf{n}}_i$  is a unit vector defined on site  $i$  of a  $d$ -dimensional hyper-cubic lattice, and the sum  $\sum_{\langle i,j \rangle}$  is taken over all nearest-neighbor bonds on the lattice. The lattice constant  $b$  will be chosen small compared to the “macroscopic” length scales of eventual physical interest, but need not be simply related to the lattice constant of the quantum antiferromagnet whose properties we wish to reproduce. Because the regularization procedure is not Lorentz invariant, the spin-wave velocity can be renormalized by the quantum fluctuations, and the constant  $c_0$  may not be exactly the same as the spin-wave velocity  $c$  at long wavelengths at  $T=0$ . Equation (2.7) is equivalent to a

Lagrangian

$$\mathcal{L} = \frac{b^d \rho_s^0}{2} \left[ \sum_i \left| \frac{d\hat{\mathbf{n}}_i}{c_0 dt} \right|^2 - \sum_{\langle i,j \rangle} \frac{|\hat{\mathbf{n}}_i - \hat{\mathbf{n}}_j|^2}{b^2} \right]. \quad (2.8)$$

The hydrodynamics associated with Eq. (2.8) is most easily worked out using the associated Hamiltonian. Passage from the Lagrangian to the Hamiltonian is somewhat subtle, because of the constraints that the  $\hat{\mathbf{n}}_i$  be unit vectors. The Hamiltonian, derived via a limiting procedure in Appendix B, is (up to an unimportant constant)

$$H = \frac{b^d}{2} \left[ \sum_i \frac{|\mathbf{M}_i|^2}{b^{2d} \chi_{\perp}^0} + \rho_s^0 \sum_{\langle i,j \rangle} \frac{|\hat{\mathbf{n}}_i - \hat{\mathbf{n}}_j|^2}{b^2} \right], \quad (2.9)$$

where  $\mathbf{M}_i b^d$  is the angular momentum on site  $i$ , and  $\chi_{\perp}^0$  is given by

$$\chi_{\perp}^0 \equiv \rho_s^0 / c_0^2. \quad (2.10)$$

If  $\hat{\mathbf{n}}_i$  is interpreted as the orientation of a rodlike rotator on lattice site  $i$ , the quantity  $\chi_{\perp}^0 b^d$  may be interpreted as its moment of inertia. The angular momentum density  $\mathbf{M}_i$  is related to  $d\hat{\mathbf{n}}_i/dt$  by

$$\mathbf{M}_i = \chi_{\perp}^0 b^d \hat{\mathbf{n}}_i \times \frac{d\hat{\mathbf{n}}_i}{dt}. \quad (2.11)$$

We shall refer to the model described by Eqs. (2.7)–(2.11) as the quantum lattice rotator model (QLRM).

The classical equation of motion for  $\mathbf{M}_i$  derived from (2.8) or from (2.9) is

$$\frac{d\mathbf{M}_i}{dt} = -\frac{\rho_s^0}{b^{2-d}} \hat{\mathbf{n}}_i \times \sum_j' (\hat{\mathbf{n}}_i - \hat{\mathbf{n}}_j), \quad (2.12)$$

where  $\sum_j'$  is the sum over the sites that are nearest neighbors to  $i$ . Equations (2.11) and (2.12), together with the constraints  $|\hat{\mathbf{n}}_i| = 1$ , determine the classical time dependence of the unit vectors  $\hat{\mathbf{n}}_i$ . Note that  $\hat{\mathbf{n}}_i \cdot \mathbf{M}_i$  is conserved by the equation of motion (2.12), while the definition (2.11) assures that  $\hat{\mathbf{n}}_i \cdot \mathbf{M}_i = 0$ , for every site of the lattice.

The Hamiltonian formulation of quantum mechanics requires that  $H$  be interpreted as an operator in the Hilbert space  $\mathcal{L}^2([S_2]^{\mathcal{N}})$ , where  $\mathcal{N}$  is the number of sites on the lattice, and  $S_2$  is the unit sphere swept out by  $\hat{\mathbf{n}}_i$ . Quantization is carried out by the usual identification

$$\mathbf{M}_i = \hat{\mathbf{n}}_i \times \frac{\hbar}{i} \frac{\partial}{\partial \hat{\mathbf{n}}_i}. \quad (2.13)$$

The time evolution determined by the Hamiltonian (2.9) is now precisely the same as the path-integral formulation using the Lagrangian (2.8), and the equilibrium density matrix  $w = Z^{-1} e^{-\beta H}$  gives the same correlation functions as the path-integral approach using the effective action (2.7). We note also that the total angular momentum

$$\mathbf{M} = \sum_i \mathbf{M}_i \quad (2.14)$$

commutes with the Hamiltonian, and, hence, it is a constant of the motion.

If  $\hat{\mathbf{n}}_i$  is treated as a classical variable, then the ground state of the system has  $\mathbf{M}_i = 0$ , and  $\hat{\mathbf{n}}_i = \hat{\mathbf{n}}$ , independent

of  $i$ . Infinitesimal deviations from the fully aligned ground state are described by a linearized version of the equations of motion (2.11) and (2.12), which give a linear spectrum of normal modes,  $\omega_k = c_0 k$ , in the limit  $k \rightarrow 0$ , with two degenerate polarization modes for each value of  $k$ .

When quantum mechanics is included in the analysis, there will be zero-point fluctuations, and the ground state will be less than fully aligned. The size of the zero-point fluctuations may be estimated from a harmonic-oscillator expansion. For dimension  $d > 1$ , one finds that the fluctuations  $\langle |\delta \hat{\mathbf{n}}_i|^2 \rangle$  are small compared to unity, provided that the dimensionless parameter

$$g_0 \equiv \text{const } \hbar c_0 b^{1-d} / \rho_s^0 \quad (2.15)$$

is sufficiently small. This suggests that there is long-range order in the ground state of an infinite system, with

$$\langle \hat{\mathbf{n}}_i \rangle = N(0) \hat{\mathbf{n}}_0, \quad (2.16)$$

where  $\hat{\mathbf{n}}_0$  is a unit vector in an arbitrary direction, and  $N(0)$  is a number between 0 and 1. For  $d=1$  there is divergence at long wavelengths, so that  $\langle \hat{\mathbf{n}}_i \rangle = 0$ , for any value of  $g_0$ . We also expect a quantum disordered phase with  $\langle \hat{\mathbf{n}}_i \rangle = 0$  at  $T=0$  for  $d > 1$ , if  $g_0$  is greater than a critical value  $g_c$ .

According to the Hohenberg-Mermin-Wagner theorem,<sup>14</sup> applied to this model, there can be no long-range order at finite temperatures, for  $d \leq 2$ . On the other hand, for  $d > 2$ , we expect to find long-range order at finite temperatures, up to a critical temperature  $T_c$  of order  $\rho_s^0 b^{d-2}$ , provided that  $g_0$  is in the range where there is long-range order at  $T=0$ . Then for  $T < T_c$ , we have

$$\langle \hat{\mathbf{n}}_i \rangle = N(T) \hat{\mathbf{n}}_0, \quad (2.17)$$

where  $\hat{\mathbf{n}}_0$  is an arbitrary unit vector, and  $N(T)$ , the average staggered magnetization, is a decreasing function of  $T$  and of  $g_0$ . The mean value  $\langle \mathbf{M} \rangle$  of the total angular momentum, however, should be 0 in all of the phases considered above. In the case of the quantum disordered ground state, which occurs at  $T=0$  for  $g_0 > g_c$ , the ground state is predicted to be rationally invariant, which means that it is actually an eigenstate of the total angular momentum with  $M^2=0$ . For  $g_0 < g_c$ , however, the ground state (in an infinite system) has spontaneously broken rotational symmetry, and it is no longer an eigenstate of  $M^2$ .

### C. Hydrodynamic behavior

#### 1. The ordered state $0 < T < T_c$ , $d > 2$

We wish to predict the long-wavelength behavior of the quantum lattice rotator model (QLRM) defined above, in the various regimes of  $T$ ,  $d$ , and  $g_0$ . To do this we employ a hydrodynamic theory which is based on the following assumptions.

(a) There exists a characteristic microscopic relaxation time  $\tau_R$  for the system, at the temperature in question, such that for small deviations from the equilibrium state, all the microscopic variables in the system will relax in a

time of order  $\tau_R$  to some quasiequilibrium values which depend only on the values of the long-wavelength Fourier components of a small number of slow "hydrodynamic variables." Typically, the hydrodynamic variables are the densities of conserved quantities, and if there is a broken continuous symmetry in the system, a set of variables that describe fluctuations in the orientation of the order parameter. In the present case, the conserved variables are the density of angular momentum, which we denote  $\mathbf{m}(\mathbf{r})$ , and the energy density, which we denote  $\varepsilon(\mathbf{r})$ . In the ordered phase of the QLRM we define an order-parameter density  $\mathbf{n}(\mathbf{r})$  as the expectation value  $\langle \hat{\mathbf{n}}_i \rangle$ , for the nonequilibrium state, averaged over some region of linear size  $l$ , centered about the point  $\mathbf{r}$ . The length scale  $l$  should be chosen larger than any characteristic length scale for equilibrium fluctuations in the order parameter, e.g., the correlation length. Then we define a local orientation of the order parameter by the unit vector,

$$\hat{\mathbf{n}}(\mathbf{r}) = \frac{\mathbf{n}(\mathbf{r})}{|\mathbf{n}(\mathbf{r})|}. \quad (2.18)$$

Of course, the magnitude  $|\mathbf{n}(\mathbf{r})|$  will be generally less than 1, due to fluctuations on the length scale smaller than  $l$ .

Note that since  $\sum_i \hat{\mathbf{n}}_i$  does not commute with the Hamiltonian (2.9), the density  $\mathbf{n}(\mathbf{r})$  is not conserved. Thus, it is reasonable to assume that a fluctuation in the magnitude of  $\mathbf{n}(\mathbf{r})$  can relax in a microscopic time  $\tau_R$ , to its quasiequilibrium value, even for fluctuations of very long length scale. On the other hand, if  $\hat{\mathbf{n}}(\mathbf{r})$  is independent of position, the energy of the equilibrium system is independent of the direction of  $\hat{\mathbf{n}}$ , so there is no reason for the value of  $\hat{\mathbf{n}}$  to relax in this case. Thus, we include  $\hat{\mathbf{n}}(\mathbf{r})$  among the independent hydrodynamic variables of the system, although the magnitude  $|\mathbf{n}(\mathbf{r})|$  is not taken explicitly into account.

(b) The second assumption of the hydrodynamic theory is that for deviations on a length scale that is large compared to a suitably chosen microscopic length  $l'$ , the time derivative of the hydrodynamic variables at any point  $\mathbf{r}$  can be expanded as a function of the hydrodynamic variables and their low-order spatial derivatives at point  $\mathbf{r}$ . A similar assumption is made for the expandability of thermodynamic functions, such as the entropy density. The laws of thermodynamics, the requirements of symmetry, and the commutation relations (or Poisson bracket relations in the classical limit) among the hydrodynamic variables then impose severe restrictions on the equations of motion.

In the present case, symmetry and thermodynamics require that for small deviations from equilibrium the entropy density  $\mathcal{S}(\mathbf{r})$  may be expanded in the form

$$\mathcal{S}(\mathbf{r}) = \mathcal{S}_0(\varepsilon) - \frac{1}{2} T^{-1} [\mathbf{m} \cdot (\tilde{\chi})^{-1} \cdot \mathbf{m} + \rho_s(T) |\nabla \mathbf{n}|^2], \quad (2.19)$$

where higher space derivatives have been omitted from the expression,  $\mathcal{S}_0(\varepsilon)$  is the equilibrium entropy density corresponding to energy density  $\varepsilon$ , when  $\mathbf{m} = \nabla \mathbf{n} = 0$ ,  $\rho_s(T)$  is by definition the macroscopic temperature-dependent stiffness constant for fluctuations in the orientation of the order parameter, and  $\tilde{\chi}$  is the angular-

momentum susceptibility tensor, whose Cartesian components may be written in the form

$$\chi_{\alpha\beta} = \chi_{\perp}(T)\delta_{\alpha\beta} - [\chi_{\perp}(T) - \chi_{\parallel}(T)]\Omega_{\alpha}\Omega_{\beta}. \quad (2.20)$$

Note that if one were to add to the Hamiltonian (2.9) a perturbation of the form  $-\mathbf{B} \cdot \mathbf{M}$ , where  $\mathbf{B}$  is a constant vector chosen perpendicular to the order-parameter direction  $\hat{\Omega}$ , then the condition that the entropy be a maximum for a given value of the total energy

$$E = \int \varepsilon(\mathbf{r}) d^d r - \mathbf{B} \cdot \int \mathbf{m}(\mathbf{r}) d^d r \quad (2.21)$$

dictates the linear response

$$\mathbf{m}(\mathbf{r}) = \chi_{\perp}(T)\mathbf{B}. \quad (2.22)$$

More generally,  $\chi_{\alpha\beta}$  may be described as the uniform paramagnetic susceptibility tensor in units where the gyromagnetic ratio ( $g\mu_{\beta}/\hbar$ ) has value unity.<sup>44</sup> (In general, the value of  $\chi_{\perp}$  is larger than  $\chi_{\parallel}$ , so that the orientation of  $\hat{\Omega}$  perpendicular to  $\mathbf{B}$  is, in fact, the stable orientation, giving the largest entropy for given  $E$  and  $\mathbf{B}$ .) We note that the absence of a term proportional to  $\mathbf{m} \cdot \hat{\Omega}$  in Eq. (2.19) is a direct consequence of the time-reversal invariance of the Hamiltonian (2.9) for the QLRM.

Equation (2.19) has precisely the form which was obtained in Eq. (6.8) of Ref. 42 for the entropy density in the Heisenberg antiferromagnet, if  $\hat{\Omega}$  is interpreted as the orientation of the staggered magnetization. (The absence of a linear coupling between  $\mathbf{m}$  and  $\hat{\Omega}$  in that case was due to the invariance under translation by one lattice constant, which interchanges the two sublattices and changes the sign of the staggered magnetization.) The commutation relation between  $\mathbf{M}$  and  $\hat{\Omega}_i$  for the QLRM also has the same form as the commutation relation between  $\mathbf{M}$  and the staggered magnetization variable in the case of the Heisenberg antiferromagnet, because the angular momentum  $\mathbf{M}$  is the generator of rotations in both cases. Then in direct analogy to Eq. (2.19) of Ref. 42, one can show that for a constrained equilibrium state where the conserved quantity  $\mathbf{M}$  is different from zero, where there is no external field  $\mathbf{B}$ , where  $\hat{\Omega}$  is perpendicular to  $\mathbf{M}$ , and where all other quantities have relaxed to their quasiequilibrium values, the order-parameter orientation will precess about the direction of  $\mathbf{M}$  at a rate given by

$$\frac{d\hat{\Omega}}{dt} = \frac{\mathbf{m}}{\chi_{\perp}(T)} \times \hat{\Omega}. \quad (2.23)$$

(This precession rate is also analogous to the Josephson equation for the rate of change of the phase of the order parameter of a superfluid or superconductor in equilibrium.)

For definiteness let us now consider small deviations from an equilibrium state with  $\mathbf{M} = 0$  and  $\hat{\Omega} \parallel \hat{\chi}$ . The unknown coefficients for the leading terms in the gradient expansion of the equations of motion are determined by Eq. (2.23) and the requirement that the total entropy of the system is a nondecreasing function of time. Repeating the procedures described in detail in Sec. 2 of Ref. 42, one

finds that, for  $\alpha = y, z$ ,

$$\frac{\partial m_{\alpha}}{\partial t} = \rho_s(T) \nabla \cdot \mathbf{V}^{\alpha}, \quad (2.24)$$

$$\frac{\partial \mathbf{V}^{\alpha}}{\partial t} = \chi_{\perp}^{-1}(T) \nabla m_{\alpha}, \quad (2.25)$$

where

$$\mathbf{V}^{\alpha} \equiv \varepsilon_{\alpha\beta\gamma} \Omega_{\beta} \nabla \Omega_{\gamma}. \quad (2.26)$$

This leads directly to a linear normal-mode spectrum

$$\omega_k = [\rho_s(T)/\chi_{\perp}(T)]^{1/2} k. \quad (2.27)$$

As shown in Ref. 42, higher terms in the gradient expansion lead to a damping rate proportional to  $k^2$ , which is negligible compared to  $\omega_k$  in the limit  $k \rightarrow 0$ . In addition to the vibrational modes, which involve the variables  $(m_y, \Omega_z)$  and  $(m_z, \Omega_y)$ , the hydrodynamic theory predicts two diffusive modes, with relaxation rates proportional to  $k^2$ , for the parallel magnetization  $m_x$  and for the heat contribution to the energy density  $\varepsilon$ .

The validity of the assumption of a finite characteristic relaxation term  $\tau_R$  for the degrees of freedom neglected in the hydrodynamic theory actually depends on some subtle aspects of the system. In actuality, there will always be some degrees of freedom, such as multiple spin-wave excitations in the antiferromagnet, which relax at a very slow rate in the limit of  $k \rightarrow 0$  (cf. the discussion in Sec. 10 of Ref. 42). It is necessary to argue that the slow modes neglected in a hydrodynamic analysis have sufficiently small phase space, or are weakly enough coupled to the hydrodynamic modes that they do not affect the results in the long-wavelength limit. A detailed analysis of the velocity and damping of spin waves in the three-dimensional Heisenberg antiferromagnet at low temperatures by Harris, Kumar, Halperin, and Hohenberg<sup>45</sup> has confirmed the validity of the hydrodynamic theory in that case.

## 2. The ordered phase at $T = 0$ , $d \geq 2$

If Eq. (2.19) is evaluated in the limit  $T \rightarrow 0$ , with the requirements that  $\mathcal{S} \rightarrow 0$  at low temperatures and  $d\mathcal{S}_0/d\varepsilon = T^{-1}$ , we find that

$$\delta\varepsilon(\mathbf{r}) = \frac{1}{2} \rho_s |\nabla \hat{\Omega}|^2 + \frac{1}{2} \mathbf{m} \cdot (\tilde{\chi})^{-1} \cdot \mathbf{m}, \quad (2.28)$$

where  $\delta\varepsilon(\mathbf{r})$  is the deviation from the energy density in the ground state of the system, and  $\rho_s$  and  $\tilde{\chi}$  are the stiffness constant and susceptibility tensor at  $T = 0$ . We see that energy density  $\varepsilon(\mathbf{r})$  is no longer an independent hydrodynamic variable of the system.

In analogy to the assumptions of the hydrodynamic theory at  $T \neq 0$ , we assume that for low-frequency motions, all other variables in the system follow adiabatically the hydrodynamic variables. Again, we assume that the energy and the equations of motion can be expanded in powers of gradients of the hydrodynamic variables, and we require that the total energy be independent of time. Again, we make use of Eq. (2.23), which still applies at  $T = 0$ , and we find the equations of motion (2.24) and (2.25) for the components of  $\mathbf{m}(\mathbf{r})$  and  $\hat{\Omega}(\mathbf{r})$  perpendicu-

lar to the average orientation  $\hat{\mathbf{n}}_0$ . We expect that  $\rho_s$  and  $\chi_\perp$  are finite at  $T=0$ , so that the elementary excitations again have a linear dispersion, with the zero-temperature spin-wave velocity  $c=(\rho_s/\chi_\perp)^{1/2}$ .

By contrast, in the limit  $T \rightarrow 0$ , we expect that  $\chi_\parallel(T) \rightarrow 0$ , for  $d > 2$ . The reason for this is that the ground state of the system is invariant under rotations about the  $\hat{\mathbf{n}}_0$  axis. Thus, in the ground state, the eigenvalue of  $\hat{\mathbf{n}}_0 \cdot \mathbf{M}$  is zero, and there is no linear response of the ground state induced by a magnetic field  $\mathbf{B}$  parallel to  $\hat{\mathbf{n}}_0$ . There do exist low-energy states, containing one or more spin-wave excitations, which have values of  $\hat{\mathbf{n}}_0 \cdot \mathbf{M}$  different from zero, and there will be a linear response at finite temperatures from the altered population of these states in the presence of  $B \neq 0$ . According to a perturbative spin-wave analysis, however, the density of states for these excitations is small at low energies, for  $d > 2$ , so that the contribution to  $\chi_\parallel(T)$  should vanish for  $T \rightarrow 0$ . In any case even for  $d=2$ , we expect that  $\chi_\parallel=0$ , at  $T=0$ , so that it is difficult to produce variations in the component of  $\mathbf{m}$  parallel to  $\hat{\mathbf{n}}$ , and this component of  $\mathbf{m}$  should not be considered as an independent hydrodynamic variable at  $T=0$ .

### 3. The disordered phase, $T > T_c$

We next consider the paramagnetic disordered phase, which occurs for  $T > T_c$ , in  $d > 2$ , and any  $T > 0$ , for  $d \leq 2$ . In this phase, there is a finite isotropic susceptibility tensor  $\chi_{\alpha\beta} = \chi(T)\delta_{\alpha\beta}$ , and there are only short-range correlations for the variable  $\hat{\mathbf{n}}_i$ , i.e., for large separations we have

$$\langle \hat{\mathbf{n}}_i \cdot \hat{\mathbf{n}}_j \rangle \sim \frac{1}{r_{ij}^{(d-1)/2}} \exp(-r_{ij}/\xi), \quad (2.29)$$

where  $r_{ij}$  is the distance between sites  $i$  and  $j$  and  $\xi$  is a correlation length which depends on the temperature.

For length scales large compared to  $\xi$ , we expect that hydrodynamics should apply. There are now four hydrodynamic variables,  $\varepsilon(\mathbf{r})$  and the three components of  $\mathbf{m}(\mathbf{r})$ . Each of these variables relaxes by a diffusive process, with relaxation rate proportional to  $k^2$  for  $k \rightarrow 0$ . The density of the order parameter  $\mathbf{n}(\mathbf{r})$  will relax at a characteristic rate  $\gamma_n$  which is finite in the limit  $k \rightarrow 0$ . The relaxation is not described exactly by a single exponential, however, and details of the relaxation are beyond the scope of a hydrodynamic theory.

The correlation length  $\xi$  diverges as  $(T - T_c)^{-\nu_d}$  for  $T \rightarrow T_c$ , in  $d > 2$ . (The exponent  $\nu_d \approx 0.70$  for  $d=3$ .) For length scales which are shorter than  $\xi$  the hydrodynamic theory cannot be used. If  $k^{-1}$  is small compared to  $\xi$  but large compared to the lattice constant or any other important microscopic length in the problem, the fluctuations in the order-parameter density  $\mathbf{n}(\mathbf{r})$  or the angular momentum density  $\mathbf{m}(\mathbf{r})$  occur on a characteristic frequency scale which can be determined, using the scaling hypothesis of dynamic critical phenomena in precisely the same way as for the Heisenberg antiferromagnet.<sup>39</sup> The result of this theory is

$$\omega_k \propto k^{d/2} \quad (2.30)$$

for  $2 < d \leq 4$ . The dynamic scaling analysis predicts also the *temperature dependence* of the order-parameter relaxation rate  $\gamma_n$  in the long-wavelength region  $k \ll \xi^{-1}$ :

$$\gamma_n \propto \xi^{-d/2}. \quad (2.31)$$

More detailed results for time-dependent correlation functions in various wavelength regimes, for  $T \rightarrow T_c$ , can be obtained from a renormalization-group analysis.<sup>46</sup> This analysis, like the dynamic scaling theory, is identical for the lattice rotator model and for the Heisenberg antiferromagnet. (Quantum mechanics plays no role in any of these analyses.)

In  $d=2$ , we find that the correlation length  $\xi$  diverges exponentially in  $1/T$ , for  $T \rightarrow 0$ , if the coupling constant  $g_0$  is in the range ( $g_0 < g_c$ ) where the ground state is ordered. The hydrodynamic theory for the disordered phase cannot be applied to the regime of wavelengths shorter than  $\xi$ , and the dynamic scaling theory developed for  $d > 2$  cannot be applied directly either. We shall argue below, however, that there should be spin-wave-like excitations with a fairly well-defined frequency, in the regime  $k \gg \xi^{-1}$ , with a spin-wave velocity that is shifted somewhat from the  $T=0$  value, by a factor which depends on  $T$  and  $k$ . The temperature dependence of the order-parameter relaxation rate, in the regime  $k \ll \xi^{-1}$ , will also be deduced from a dynamic scaling argument which matches the results at the scale  $k \approx \xi^{-1}$ . Again, there will be nothing in our analysis to suggest a difference between the quantum lattice rotator model and the Heisenberg antiferromagnet. By definition, the nonlinear  $\sigma$  model has identical characteristics to the QLRM, with appropriate choice of parameters, since the QLRM is just a particular regularization of the QNL $\sigma$ M, and the properties of the QNL $\sigma$ M are supposed to be independent of details of the regularization.

### 4. The quantum disordered phase ( $T=0$ )

The hydrodynamic theory cannot be applied to the quantum disordered phase, which occurs in the QLRM for  $g_0 > g_c$ , in  $d > 1$ , and for all values of  $g_0$  at  $d=1$ . The ground state is an eigenstate of  $M^2$ , with  $M^2=0$ , and it is separated by an energy gap  $\Delta$  from all other states of the system. Thus, the uniform susceptibility  $\chi$  is zero in the ground state, and the energy  $E$  cannot be expanded in powers of  $m$ .

The existence of an energy gap is easily seen in the limit where  $\rho_s^0=0$ , in the Hamiltonian (2.9), with  $\chi_\perp^0$  held fixed ( $g_0=\infty$ ). Then the ground-state wave function is the state where  $M_i^2=0$ , for every site  $i$ . Excited states may be denoted by  $|\{l_i, m_i\}\rangle$ , where  $l_i=0, 1, 2, \dots$  and  $-l_i \leq m_i \leq l_i$  are the angular momentum quantum numbers of the  $i$ th site. The lowest excited state, which has degeneracy  $3N$ , is a state where one of the sites is a "triplet," with  $b^{2d}M_j^2=2\hbar^2$  for one particular lattice site  $j$ , and  $M_i^2=0$  elsewhere. The energy "gap" associated with this state is  $\hbar^2/\chi_\perp^0$ .

For  $\rho_s^0 \neq 0$  ( $g_0 < \infty$ ), the degeneracy of the excited states is broken, and the energy gap will be diminished. It is believed, however, that the gap remains open until

$g_0 = g_c$ , where the transition to the ordered phase occurs. The behavior of the system near the point  $g_0 = g_c$  will be discussed further below.

The nature of the quantum disordered phase of the Heisenberg antiferromagnet at  $T=0$  is the subject of considerable debate,<sup>31,33,35</sup> as was mentioned earlier in our introduction. Only in the case of  $d=1$  is there general agreement about the properties of the system. It appears that for chains with integer spin the ground state of the antiferromagnet has static and dynamic properties that coincide with the ones described above for the QLRM, or the QNL $\sigma$ M, but this is not the case for  $\frac{1}{2}$ -integer spins. It is believed that the long-wavelength properties of the  $\frac{1}{2}$ -integer spin chains are identical to the properties of a modification of the QNL $\sigma$ M, in which the action is multiplied by  $(-1)^n$ , where  $n$  is the topological "skyrmion number" of space-time configuration. It is known in the case of spin- $\frac{1}{2}$ , and believed to be true for all  $\frac{1}{2}$ -integer spin chains, that the staggered correlation function  $(-1)^{i-j} \langle \mathbf{S}_i \cdot \mathbf{S}_j \rangle$  falls off as the inverse of the separation  $|i-j|$  for large separations, so the system has neither long-range order nor an energy gap in its ground state.

### III. QUANTUM TRANSITION REGION

We now analyze the equilibrium properties of the QNL $\sigma$ M using the renormalization-group equations derived in Appendix C. The equations to one-loop order are

$$\frac{dg}{dl} = (1-d)g + \frac{K_d}{2} g^2 \coth(g/2t) \quad (3.1a)$$

and

$$\frac{dt}{dl} = (2-d)t + \frac{K_d}{2} g t \coth(g/2t). \quad (3.1b)$$

Here,  $e^l$  is the length rescaling factor,  $K_d^{-1} = 2^{d-1} \pi^{d/2} \Gamma(d/2)$ , and the initial values of the dimensionless coupling constant  $g(l)$  and temperature scale  $t(l)$  are  $g_0 = \hbar c \Lambda^{d-1} / \rho_s^0$  and  $t_0 = k_B T \Lambda^{d-2} / \rho_s^0$ . As pointed out in Appendix C,  $g/t = \beta \hbar c \Lambda$  is the dimensionless "slab thickness" of  $(d+1)$ -dimensional QNL $\sigma$ M in the time-like direction, and obeys the simple recursion relation

$$d(g/t)/dl = -g/t. \quad (3.2)$$

In Sec. V, we shall discuss the two-loop extension of these equations in the regime in which the  $T=0$  state has LRO. For the moment we shall use Eqs. (3.1) and (3.2) to discuss the qualitative nature of the phase diagram.

Note that in the limit  $T \rightarrow 0$ , Eq. (3.1a) is nothing but the one-loop recursion relation of the  $(d+1)$ -dimensional nonlinear  $\sigma$  model. Similarly in the high-temperature limit Eq. (3.1b) goes over to the one-loop recursion relation of the classical  $d$ -dimensional nonlinear  $\sigma$  model.

The renormalization-group flows are easy to construct from Eqs. (3.1). In fact, it is possible to obtain exact closed-form solutions of these equations for arbitrary dimension  $d$  using Eq. (3.2). At  $T=0$ , there is a nontrivial fixed point  $g = g_c$  for  $d > 1$ , where  $g_c$  is given by

$$g_c = \frac{2}{K_d} (d-1). \quad (3.3a)$$

This describes a quantum phase transition which has the critical exponents of a classical  $(d+1)$ -dimensional Heisenberg model. For  $d \leq 2$ , there are no finite-temperature fixed points, while for  $d > 2$  there is a fixed point at

$$t_c = (d-2)/K_d \quad (3.3b)$$

describing a classical finite-temperature  $d$ -dimensional ordering transition.

The renormalization-group flows for  $d > 2$  are shown in Fig. 2(a). When  $T=t=0$ , the fixed point at  $g_c$  controls a transition from the Néel state at small  $g$  to a quantum disordered phase at large  $g$ . As discussed earlier,  $g$  plays the role of  $1/S$  in Fig. 1. When temperature is reduced for fixed  $g < g_c$ , there is a finite-temperature phase transition along the heavy separatrix controlled by the thermal fixed point at  $g=0$ ,  $t=t_c$ . The shaded region has long-range Néel order, controlled by the fixed point at the origin. As  $d \rightarrow 2^+$ , this thermal fixed point merges with the fixed point at the origin.

In the remainder of this paper we shall concentrate on  $d=2$ . The renormalization-group flows are shown for  $d=2$  in Fig. 2(b), where we have used the definitions  $\bar{g} \equiv g/g_c$  and  $\bar{t} \equiv t/2\pi$ . In this case the region of Néel order collapses to a line at  $t=0$ , which terminates at  $g_c$ , where  $g_c = 4\pi$  from the one-loop approximation. For  $g > g_c$  at  $T=0$  there is a transition to a disordered phase with a gap

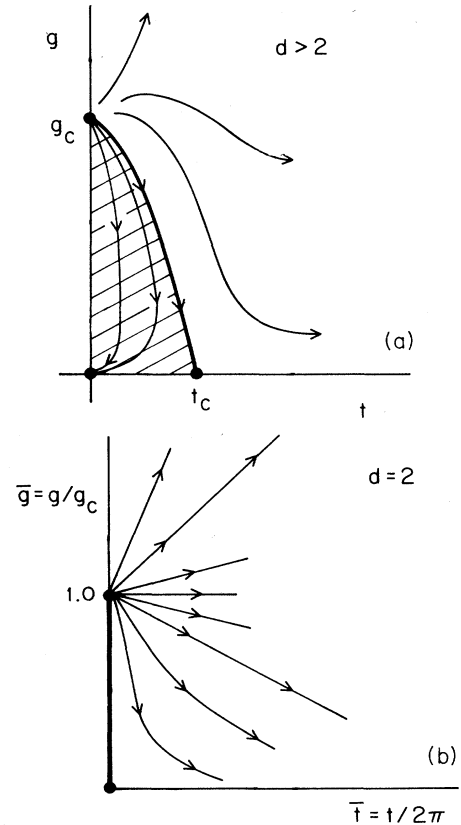


FIG. 2. (a) Renormalization-group flows for the QNL $\sigma$ M for  $d > 2$ . (b) Renormalization-group flows for the QNL $\sigma$ M for  $d=2$ .

in the excitation spectrum, just as for  $d > 2$ . Although the system is disordered at all finite temperatures, we can nevertheless identify three regions separated by crossover lines. These regions are characterized by the behavior of the correlation length as a function of temperature.

The correlation length can be calculated from our recursion relations by integrating them until the renormalized correlation length  $\xi(l) = e^{-l}\xi$  equals the lattice constant. For  $\bar{g} < 1 + \bar{t}$ ,  $t(l)$  grows faster than  $g(l)$  and it suffices to choose  $l^*$  such that  $t(l^*) = 2\pi$ . One-loop results are only weakly dependent on the precise matching condition. Although this method cannot give correctly the amplitudes of singular quantities, it does shed considerable light on the phase diagram. Using the exact solutions of Eqs. (3.1) and (3.2) for the case  $d=2$ , we obtain for  $\xi = ae^{l^*}$ ,

$$\xi^{-1} = \left( \frac{\bar{t}_0}{a\bar{g}_0} \right) \sinh^{-1} \{ \sinh(\bar{g}_0/\bar{t}_0) \exp[-(1-\bar{t}_0)/\bar{t}_0] \}. \quad (3.4)$$

The prefactor  $\bar{t}_0/a\bar{g}_0 = \sqrt{2/\pi}(k_B T/\hbar c)$  is not explicitly dependent on  $a$ . Other choices of the matching condition would change the coefficient  $(2/\pi)^{1/2}$ .

It is easy to show that for the regime  $1 + \bar{t} > \bar{g}_0 > 1 - \bar{t}$ ,  $\xi$  is asymptotically given by  $\xi = \text{const}(\hbar c/k_B T)$ . At precisely  $\bar{g}_0 = 1$  we find, within our approximation, that as  $T \rightarrow 0$ ,

$$\xi(\bar{g}_0 = 1) = 1.1 \frac{\hbar c}{k_B T}. \quad (3.5)$$

In fact, this is a far more general result than our method of derivation suggests. Precisely at  $g_0 = g_c$  the system will behave like a three-dimensional classical spin system at its critical point, for length scales less than the effective "slab thickness"  $\beta\hbar c$ . The order will be broken up by two-dimensional fluctuations on larger scales, so we conclude that for  $g_0 = g_c$ ,

$$\xi = C_Q \frac{\hbar c}{k_B T} \quad (3.6)$$

as  $T \rightarrow 0$ , where  $C_Q$  is a universal constant of order unity.

When  $\bar{g}_0 < 1 - \bar{t}$  it is easy to show from Eq. (3.4) that the correlation length ultimately diverges exponentially as  $T \rightarrow 0$ . In this regime one finds within the one-loop approximation that

$$\xi \approx 0.9 \left( \frac{\hbar c}{k_B T} \right) \exp(2\pi\rho_s/k_B T), \quad (3.7a)$$

where  $\rho_s$  is the actual spin-stiffness constant at  $T=0$ , renormalized by the quantum fluctuations. We find that

$$\rho_s = \rho_s^0(1 - \bar{g}_0), \quad (3.7b)$$

which is shown in Appendix C to be the renormalized spin stiffness at  $T=0$  within the one-loop approximation. Since  $\rho_s$  vanishes as  $\bar{g}_0 \rightarrow 1$ , it is clear that proximity to the  $T=0$  fixed point at  $g_c$  can greatly reduce the rate of growth of  $\xi$ . The prefactor  $\hbar c/k_B T$  in Eq. (3.7a) is the thermal de Broglie wavelength of the spin waves (divided by  $2\pi$ ).

Although the result for the preexponential factor ob-

tained in the one-loop approximation will change when we consider two-loop corrections in the renormalized classical regime, the one-loop expression for the correlation length is nevertheless rather interesting. If one takes the limit  $\bar{g}_0/\bar{t}_0 \rightarrow 0$  in Eq. (3.4), with  $\bar{t} \ll 1$ , one obtains the one-loop expression for correlation length in the *classical* 2D nonlinear  $\sigma$  model, which we may write as

$$\xi = 0.36a \exp(2\pi\rho_s^0/k_B T). \quad (3.7c)$$

Qualitatively we learn from Eqs. (3.7) that for the quantum model,  $\xi$  diverges just as it would in the corresponding classical model except for two facts: (a)  $\rho_s$  is the *renormalized* spin-stiffness constant and contains the effect of quantum fluctuations, and (b) the short-wavelength cutoff is the thermal de Broglie wavelength  $\hbar c/k_B T$  rather than a constant times the lattice spacing  $a$ .

We now consider the quantum disordered regime  $\bar{g} > 1 + \bar{t}$ . In this regime the solution of Eqs. (3.1) and (3.2) shows that  $g(l)$  grows faster than  $t(l)$ , and it is convenient to choose  $l^*$  such that  $\bar{g}(l^*) = 2$ ; i.e.,  $g(l^*) = 2g_c$ . This yields an implicit equation for  $e^{l^*}$ . As  $\bar{t}_0 \rightarrow 0$  ( $T \rightarrow 0$ ),  $\xi$  is approximately given by the following expression:

$$\xi \approx \frac{a\bar{g}_0/2}{(\bar{g}_0 - 1) + \bar{t}_0 \exp[-4(\bar{g}_0 - 1)/\bar{t}_0]}. \quad (3.8)$$

Note that the corrections to the  $\bar{t}_0 = 0$  value vanish exponentially fast as  $\bar{t}_0 \rightarrow 0$ . Thus, we do not expect  $\xi$  to vary much in this regime as  $T \rightarrow 0$ . This exponential dependence with respect to temperature is the signature of a gap  $\Delta \sim \bar{g}_0 - 1$  in the excitation spectrum for  $\bar{g}_0 > 1$ .

The overall phase diagram is summarized in Fig. 3. The central *quantum critical* region is controlled by the

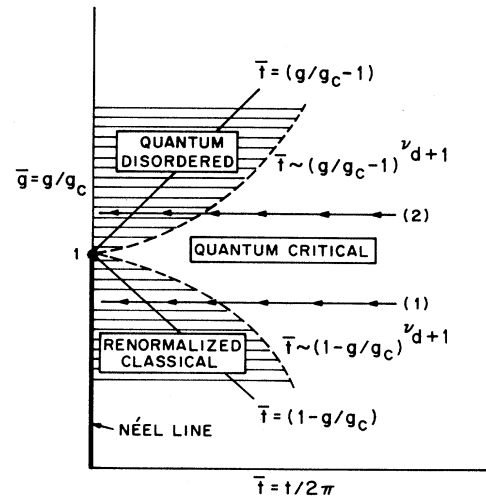


FIG. 3. Crossover diagram for the QNL $\sigma$ M at  $d=2$ . The lines marked (1) and (2) are two possible experimental paths for which the staggered spin-spin correlation length will behave very differently. As the temperature is lowered along path (2) the correlation length will become essentially temperature independent as it crosses the crossover line. Along path (1) the correlation length will diverge exponentially once it crosses the crossover line.

$T=0$  fixed point at  $g_c$ . In this region we have quite generally  $\xi \propto \hbar c/k_B T$  (at low temperatures). The *renormalized classical* region is separated from the quantum critical region by the crossover line  $\bar{g} = 1 - \bar{t}$ . In this regime  $\xi$  diverges exponentially as  $T \rightarrow 0$ . The *quantum disordered* region is separated from the quantum critical region by the crossover line  $\bar{g} = 1 + \bar{t}$ . In this regime  $\xi$  becomes independent of temperature as  $T \rightarrow 0$ . Thus, from experiments carried out at finite temperatures it should be possible to determine the nature of the  $T=0$  state.

The qualitative features of the phase diagram shown in Fig. 3 transcend the one-loop method described above. However, there should be quantitative corrections as follows: The  $(2+1)$ -dimensional QNL $\sigma$ M must have a phase transition to the disordered state at  $T=0$ , at some value  $g_c$  of the dimensionless coupling constant. The exponent  $\nu_{d+1} \equiv \nu_3$  should be the same as that of Heisenberg model in three dimensions which is  $\nu_3 \approx 0.7$ , rather than the value  $\nu_3 = 1$  that one obtains from a one-loop analysis of the nonlinear sigma model. The Lorentz invariance of the model at  $T=0$ , when an appropriate cutoff is used, implies a well-defined excitation spectrum which has the dispersion relation  $\omega_k = c[k^2 + \xi(T=0)^{-2}]^{1/2}$ , in the quantum disordered state. Thus, there is an energy gap  $\Delta = \hbar c \xi(T=0)^{-1} \propto (g_0/g_c - 1)^{\nu_3}$ .

Next, consider the crossover lines shown in Fig. 3. For  $g_0 > g_c$ , the effect of finite temperature will be felt when one exceeds a crossover temperature  $T_x \approx \Delta/k_B \propto (g_0/g_c - 1)^{\nu_3}$ . For  $g_0 < g_c$ , we obtain the crossover temperature by first defining, following Josephson,<sup>36</sup> a correlation length  $\xi_J \approx (\hbar c/\rho_s)^{1/(d-1)}$  which separates, at  $T=0$ , the long-wavelength antiferromagnetic magnons from the shorter-wavelength critical fluctuations important near  $g_c$ . We expect that  $\xi_J \sim (1 - g_0/g_c)^{\nu_3}$  near  $g_c$ , and obtain a crossover temperature  $T_x' \sim (1 - g_0/g_c)^{\nu_3}$  by setting  $\xi_J$  equal to the thermal length  $\hbar c/k_B T \approx \xi(g_c, T)$ . To one-loop order,  $c$  is not renormalized at zero temperature due to Lorentz invariance. A more accurate calculation should lead to a finite renormalization of  $c$  because of the non-Lorentz invariance of our cutoff procedure. In either case, it is clear that  $c$  remains finite even though  $\rho_s$  vanishes at  $g_c$ . This necessarily implies that the uniform susceptibility vanishes at the same rate as  $\rho_s$  does as  $g \rightarrow g_c^-$ . From the arguments given above one obtains the crossover lines shown by the dashed curves in Fig. 3 which differ from the lines obtained from a one-loop approximation simply because  $\nu_3 = 0.7$  instead of 1 as in the one-loop approximation.

To proceed further within the one-loop approach, we must determine the coupling constant  $\bar{g}_0$ . If we choose  $\bar{g}_0 < 1$  and set  $T=0$ , then the spin stiffness  $\rho_s$  and the magnetic susceptibility  $\chi_\perp$  approach finite values in the long-wavelength limit. From the defining relation for  $g$  (see Appendix C), we have then, for  $d=2$ ,

$$\chi_\perp = \rho_s/c^2 = \lim_{l \rightarrow \infty} [\hbar \Lambda e^{-l}/cg(l)]. \quad (3.9)$$

If one integrates Eq. (3.1a), at  $T=0$ , one finds that

$$g(l) = 4\pi\bar{g}_0 e^{-l}/[1 - \bar{g}_0(1 - e^{-l})]. \quad (3.10)$$

Hence, from Eq. (3.9), we obtain

$$\bar{g}_0 = \frac{1}{1 + (4\pi\chi_\perp c/\hbar\Lambda)}. \quad (3.11)$$

Thus, in principle, it is possible to obtain  $\bar{g}_0$  from experimentally measured values of  $\chi_\perp$  and  $c$ . To describe an underlying square lattice with lattice constant  $a$  when  $d=2$ , one can take  $\Lambda a$  equal to  $\sqrt{2}\pi$ . This particular choice conserves the area of the Brillouin zone for the antiferromagnetically ordered state. In our earlier paper<sup>5</sup> we used spin-wave theory to determine  $\chi_\perp$  and adjusted the spin-wave velocity  $c$  in order to get a fit to the finite-temperature correlation lengths obtained in the experiment.<sup>4</sup> We chose this particular route because no reliable experimental value for  $\chi_\perp$  at  $T=0$  is known. Similarly, from neutron scattering it has not yet been possible to determine  $c$ . Initially, it was estimated from experiments<sup>4</sup> that  $\hbar c \geq 0.4$  eV Å. This bound is now improved<sup>38</sup> to be  $\hbar c \geq 0.6$  eV Å. From light scattering measurements, however, Lyons *et al.*<sup>37</sup> estimate  $\hbar c \approx 0.74$  eV Å. However, it was also necessary to employ an approximate spin-wave theory to extract  $\hbar c$  from the light scattering data, and there are important differences between the observed line shape and the line shape predicted by the theory. The details of our determination of  $\bar{g}_0$  for  $\text{La}_2\text{CuO}_4$  are given in Sec. VB.

#### IV. THE CLASSICAL LATTICE O(3) ROTATOR MODEL AND DYNAMICAL SCALING

Before going further with our discussion of quantum-mechanical models, it will be helpful to examine the properties of the lattice rotator model, defined by Eqs. (2.8) or (2.9) in the classical limit ( $\hbar \rightarrow 0$ ). We denote this system the classical lattice O(3) rotator model (CLRM). As discussed in Sec. III, this is the correct physical description of quantum antiferromagnets at long wavelengths, provided  $g < g_c$ .

Equilibrium properties of the lattice version of the classical nonlinear  $\sigma$  model have been studied in the past by Monte Carlo simulations.<sup>47-49</sup> An alternate approach, which we believe may be more efficient, is to implement a molecular-dynamics simulation of the CLRM. In either case, a classical simulation can handle lattices that are significantly larger than would be feasible in direct simulations of a quantum antiferromagnet. In Sec. V we shall employ a renormalization-group analysis to relate the equilibrium properties of the quantum systems to those of the CLRM and thereby make predictions for the quantum system using results of previous Monte Carlo simulations for the classical model.<sup>47-49</sup>

The dynamics of quantum antiferromagnets at long wavelengths and low frequencies are also described by the dynamical properties of the CLRM in the renormalized classical regime of Fig. 3. After summarizing the known static properties of the CLRM in this section we shall investigate the dynamics in the regime of low, but nonzero temperatures.

Most of the equilibrium properties of the CLRM, such as the equal-time correlation functions for the order pa-

parameter  $\langle \hat{\mathbf{n}}_i, \hat{\mathbf{n}}_j \rangle$  may be directly obtained from a lattice implementation of the classical nonlinear  $\sigma$  model, in which the angular momentum variables  $\mathbf{M}_i$  are omitted from the description, and averages are taken over the orientations  $\hat{\mathbf{n}}_i$ . The specific heat of this classical nonlinear  $\sigma$  model differs from that of CLRM only by a constant,  $k_B$  per lattice site, which arises from the kinetic-energy term proportional to  $M_i^2$ , in the CLRM. Other thermodynamic functions, such as the free energy, are likewise related in the two models by a simple transformation.

#### A. Uniform susceptibility in the classical limit

There are additional equilibrium quantities of the CLRM that are only indirectly related to the classical nonlinear  $\sigma$  model. For example, the angular momentum susceptibility tensor  $\tilde{\chi}$  has no direct definition in the nonlinear  $\sigma$  model. However, it is easy to show that in the CLRM,  $\tilde{\chi}$  is directly related to the average of the moment of inertia tensor on the individual lattice sites, so that

$$\chi_{\alpha\beta} = \chi_{\perp}^0 (\delta_{\alpha\beta} - \langle \Omega_{i\alpha} \Omega_{i\beta} \rangle). \quad (4.1)$$

The proof is given most easily if we consider the CLRM via the limiting procedure discussed in Appendix B: the constraints  $|\hat{\mathbf{n}}_i| = 1$  are replaced by a potential energy  $V(|\hat{\mathbf{n}}_i|)$  which has a steep minimum at  $|\hat{\mathbf{n}}_i| = 1$ , while the kinetic-energy term in (2.9) is replaced by  $b^d \sum_i |\mathbf{p}_i|^2 / (2\chi_{\perp}^0)$ , where  $\mathbf{p}_i$  is the linear momentum conjugate to  $\hat{\mathbf{n}}_i$ . Then, using the definition  $\mathbf{M}_i = \hat{\mathbf{n}}_i \times \mathbf{p}_i$ , we have

$$\begin{aligned} k_B T \chi_{\alpha\beta} &= b^d \sum_j \langle M_{i\alpha} M_{j\beta} \rangle \\ &= b^d \epsilon_{\alpha\gamma\eta} \epsilon_{\beta\gamma'\eta'} \sum_j \langle p_{i\eta} p_{j\eta'} \Omega_{i\gamma} \Omega_{j\gamma'} \rangle. \end{aligned} \quad (4.2)$$

Equation (4.1) then follows from the facts that there are no correlations between the momenta and the coordinates in thermal equilibrium, and

$$\langle p_{i\eta} p_{j\eta'} \rangle = (k_B T \chi_{\perp}^0) b^{-d} \delta_{ij} \delta_{\eta\eta'}.$$

#### B. Order-parameter correlation functions

It will be convenient to introduce an order-parameter normalization factor  $N_0$ , so that the order parameter of the system is defined to be  $N_0 \hat{\mathbf{n}}_i$ . (When we apply our results to the quantum antiferromagnet,  $N_0$  will take into account the reduction in the order at  $T=0$ , due to quantum fluctuations.) Then we define the order-parameter correlation functions  $S(\mathbf{k})$  and  $S(\mathbf{k}, \omega)$  as the Fourier transforms of expectation values  $N_0^2 \langle \hat{\mathbf{n}}_i(t) \cdot \hat{\mathbf{n}}_j(0) \rangle$ ; viz.

$$S(\mathbf{k}) = b^d \sum_i e^{-i\mathbf{k} \cdot \mathbf{r}_{ij}} N_0^2 \langle \hat{\mathbf{n}}_i \cdot \hat{\mathbf{n}}_j \rangle, \quad (4.3)$$

$$S(\mathbf{k}, \omega) = b^d \int_{-\infty}^{\infty} dt \sum_i e^{i\omega t - i\mathbf{k} \cdot \mathbf{r}_{ij}} N_0^2 \langle \hat{\mathbf{n}}_i(t) \cdot \hat{\mathbf{n}}_j(0) \rangle, \quad (4.4)$$

where  $\mathbf{r}_{ij}$  is the spatial separation between lattice sites  $i$

and  $j$  and the expectation values are evaluated at a single time unless explicit time variables are given [when (4.3) and (4.4) are probed via neutron scattering in quantum antiferromagnets,  $\mathbf{k}$  represents the deviation from the wave vector of the incipient antiferromagnetic order].

For  $d=2$  and  $T \neq 0$ , the order-parameter correlation function should fall off exponentially at large distances, as in Eq. (2.29). This implies that the Fourier transform  $S(\mathbf{k})$  has a pair of simple poles on the imaginary axis, at  $k = \pm i\xi^{-1}$ .

The temperature dependence of  $\xi$ , for  $T \rightarrow 0$ , should be given correctly by the two-loop renormalization-group analysis of the classical nonlinear  $\sigma$  model (see further discussion in Sec. V). This predicts that for  $T \rightarrow 0$  in the CLRM,<sup>50</sup>

$$\xi \sim B_{\xi} b \frac{e^{2\pi/t_0}}{2\pi/t_0}, \quad (4.5)$$

where  $t_0$  is the dimensionless bare coupling constant

$$t_0 = k_B T / \rho_s^0. \quad (4.6)$$

The dimensionless constant  $B_{\xi}$  cannot be determined by the two-loop theory, but it can be determined in principle by fitting the results of a computer simulation to formula (4.5). This was done by Shenker and Tobochnik and others,<sup>47-49</sup> who found

$$B_{\xi} \approx 0.01, \quad (4.7)$$

with an estimated uncertainty of order  $\pm 30\%$ . The renormalization-group analysis also predicts

$$S(k=0) = B_s \xi^2 t_0^2 N_0^2 / (2\pi)^2, \quad (4.8a)$$

where  $B_s$  is another dimensionless constant, which is not determined by the two-loop renormalization group, but which may be determined in principle by a computer simulation. The numerical results of Shenker and Tobochnik imply

$$B_s \approx \frac{0.018}{B_{\xi}^2}. \quad (4.8b)$$

We may note, also, that because there is no long-range order at  $T \neq 0$  for  $d=2$ , Eq. (4.1) becomes simply

$$\chi_{\alpha\beta} = \frac{2}{3} \chi_{\perp}^0 \delta_{\alpha\beta}. \quad (4.9)$$

In Appendix D, we show using a simple momentum shell renormalization group<sup>22</sup> that  $S(k)$  assumes the scaling form

$$S(k) = S(k=0) f(k\xi),$$

with

$$f(x) \approx \frac{1 + \frac{1}{2} \ln(1+x^2)}{1+x^2}. \quad (4.10)$$

A more accurate form for the scaling function  $f(x)$  might introduce a coefficient of order unity which multiplies the logarithmic term. In any case, we note that

$$f(x) \approx \ln x / x^2 \quad (4.11)$$

for large  $x$ , so that  $S(k)$  for the classical model actually

vanishes as  $t_0 \rightarrow 0$  for  $k \neq 0$ , according to

$$S(k) \approx \frac{2t_0 N_0^2}{k^2} \quad (\text{classical}). \quad (4.12a)$$

For a quantum antiferromagnet, residual zero-point motion leads to a nonzero limit as  $t_0 \rightarrow 0$  when  $\hbar c/k_B T > k^{-1}$ ,

$$\lim_{t_0 \rightarrow 0} S(k) \approx \frac{\hbar c N_0^2}{k \rho_s}. \quad (4.12b)$$

Although there are not yet dynamic renormalization-group calculations appropriate to the CLRM in  $d=2$ , it is natural to suppose that  $S(k, \omega)$  satisfies a similar *dynamic* scaling hypothesis, which may be expressed as

$$S(k, \omega) \sim \bar{\omega}_0^{-1} S(k) \Phi(k\xi, \omega/\bar{\omega}_0) \quad (4.13)$$

where  $\bar{\omega}_0$  is a characteristic frequency for  $k=0$ , and  $\Phi$ , by definition, must satisfy

$$\int_{-\infty}^{\infty} \Phi(x, y) \frac{dy}{2\pi} = 1, \quad (4.14)$$

for any value of  $x$ .

We shall argue in the following subsection that the characteristic frequency  $\bar{\omega}_0$  must have the form

$$\bar{\omega}_0 \sim \text{const} \left[ \frac{t_0}{2\pi} \right]^{1/2} \xi^{-1} \left[ \frac{\rho_s^0}{\chi_{\perp}^0} \right]^{1/2} \quad (4.15)$$

in the limit  $(\xi/b) \rightarrow \infty$ . We may choose the constant in (4.15) to be unity if we wish, since we have not specified the width of the function  $\Phi(0, y)$ . The essential feature of the argument is that for  $k\xi$  large, we expect moderately well-defined spin waves whose frequency should be given, at least approximately by the results of spin-wave hydrodynamics in an ordered phase [cf. Eq. (2.27)],

$$\omega_k \approx [\rho_s(k)/\chi_{\perp}]^{1/2} k, \quad (4.16)$$

where  $\rho_s(k)$  is the temperature-dependent renormalized spin stiffness constant on a length scale equal to  $k^{-1}$ , and  $\chi_{\perp}$  is the renormalized angular momentum susceptibility on the same length scale. Equation (4.15) can then be obtained by setting  $k \approx \xi^{-1}$ , and using the renormalization-group results, derived in Appendix D, that  $\rho_s(k = \xi^{-1}) \approx t_0 \rho_s^0 / 2\pi$  and  $\chi_{\perp} \approx \frac{2}{3} \chi_{\perp}^0$ .

The precise form of the function  $\Phi(x, y)$  is not known at present. In principle, it may be determined by fitting Eq. (4.13) to a molecular-dynamics simulation of the CLRM. The arguments in Sec. IVC, however, will enable us to predict the form of  $\Phi(x, y)$  for large values of  $x$ .

### C. Justification for the dynamic scaling hypothesis

In order to justify the dynamic scaling hypothesis for the CLRM, let us consider first a length scale  $\lambda \equiv be^l$  in the intermediate range, which satisfies the inequalities  $b \ll \lambda \ll \xi$ . In this range, the running coupling constant discussed in Appendix D,  $t(l) \equiv k_B T / \rho_s(l)$ , which enters the static renormalization-group equations for the classical nonlinear  $\sigma$  model in  $d=2$ , is small compared to the

value  $t(l^*) \approx 2\pi$ , which occurs at  $\lambda = \xi$ . Therefore the order-parameter fluctuations in a wave-vector interval  $\lambda^{-1} < k < 2\lambda^{-1}$  are not particularly large. If we divide the lattice into a set of regions of linear size  $\lambda$ , and if we denote the average of the order parameter in the region about point  $\mathbf{r}$  at time  $t$  by  $\mathbf{n}_{\lambda}(\mathbf{r}, t)$  then the direction of  $\mathbf{n}_{\lambda}$  should not differ too much from one cell to the next.

We expect that on the length scale  $\lambda$ , we can use, at least approximately, the same type of hydrodynamic analysis as we used in Sec. II to discuss the spin waves in the ordered phase at finite temperatures, for  $d > 2$ . This means that for  $k \approx 1/\lambda$  there should be well-defined spin-wave excitations, with a frequency given by

$$\omega_k \approx [\rho_s(l)/\chi_{\perp}(l)]^{1/2} k, \quad (4.17)$$

where  $\chi_{\perp}(l)$  is a locally defined angular-momentum susceptibility in the direction perpendicular to  $\mathbf{n}_{\lambda}(\mathbf{r})$ . As discussed above, we would clearly expect that  $\chi_{\perp}(l)$  is in the range  $\frac{2}{3} \chi_{\perp}^0 \leq \chi_{\perp}(l) \leq \chi_{\perp}^0$ . In Appendix D, we show that  $\chi_{\perp}(k = \xi^{-1}, t_0) \approx \frac{2}{3} \chi_{\perp}^0 + \text{const} t_0^2$  for small  $t_0$ , so to an excellent approximation, we can simply set

$$\chi_{\perp}(l) \approx \frac{2}{3} \chi_{\perp}^0. \quad (4.18)$$

Using the methods of Appendix D, it is easy to show that  $\rho_s(l) \sim t_0 \rho_s^0$  is only a weak function of  $k\xi$ , for  $k\xi \gg 1$ , so that there is a well-defined spin-wave velocity

$$\tilde{c}(l) \approx [3\rho_s(l)/2\chi_{\perp}^0]^{1/2} \quad (4.19)$$

which varies slowly as a function of  $k\xi$  in this regime.

In order for the hydrodynamic theory to apply with the renormalized spin-stiffness constant  $\rho_s(l)$ , it is necessary that the fluctuations responsible for the renormalization of  $\rho_s$  occur on a time scale short compared to  $\omega_k^{-1}$ . Since the renormalization of  $\rho_s$  comes primarily from fluctuations with wave vector  $k'$  large compared to  $k$ , the characteristic frequency of these fluctuations will indeed be large compared to  $\omega_k$ .

In so far as the short-wavelength fluctuations can follow adiabatically the fluctuations on length scale  $k^{-1}$ , these fluctuations will not lead to a very large damping of the spin-wave motion. The dominant damping of the spin waves with wave vector  $k$  will most likely arise from interaction with other spin waves of comparable wave vector. The dimensionless measure of the coupling to these spin waves is given by the coupling constant  $t(l)$ . Thus, it seems reasonable to suppose that the ratio of the spin-wave damping rate  $\gamma_k$ , to the frequency  $\omega_k$ , should be proportional to some positive power of  $t(l)$ . A matching calculation like that in Appendix D gives  $t(l) \approx [1 + \frac{1}{2} \ln(1 + k^2 \xi^2)]^{-1} \approx 1/\ln k \xi$  for  $k \xi \gg 1$ . Thus, for large values of  $k \xi$ , we expect

$$\frac{\gamma_k}{\omega_k} \sim \left[ \frac{1}{1 + \ln(k \xi)} \right]^w, \quad (4.20)$$

where  $w$  is an unknown exponent.

The ratio  $\gamma_k/\omega_k$  will become of order unity as the wave vector of the spin wave decreases to the vicinity of  $\xi^{-1}$ . At the same time, as  $t(l)$  becomes larger, the contribution to the correlation function  $S(k, \omega)$  from multiple spin-

wave excitations becomes significant. Since the short-wave excitations can still be assumed to follow the motion adiabatically, the form of  $S(k, \omega)$  should be determined in principle by a self-consistent calculation of interacting spin waves, on the length scale  $\xi$ , with a characteristic frequency that matches onto the spin-wave spectrum (4.18), for  $k > \xi^{-1}$ . When  $k = \xi^{-1}$ , we should find a characteristic frequency  $\omega_{\xi^{-1}}$  of order  $\tilde{c}(l)\xi^{-1}$ , with  $\tilde{c}(l) \approx (3k_B T/4\pi\chi_{\perp}^0)^{1/2}$ . Since the order parameter is not conserved, the relaxation rate at  $k=0$  should not be very different from  $k = \xi^{-1}$ . Hence, we are led to the result (4.15) for the characteristic frequency of  $S(k, \omega)$  at  $k=0$ .

In view of the above discussion, we can put the following constraint on the dimensionless function  $\Phi(x, y)$ . For large values of  $x$ ,  $\Phi(x, y)$  should have peaks at the values  $y \approx \pm (\frac{3}{2})^{1/2} x (\ln x)^{1/2}$ , with a width that is smaller than this by some power of  $1/(\ln x)$ . (Here we have chosen the constant on the right-hand side of (4.15), equal to unity.)

#### D. Relaxation of the angular momentum density

Because the total angular momentum is conserved, the angular momentum density  $\mathbf{m}(r)$  should relax according to a diffusion law, with relaxation rate  $D_m k^2$ , for  $k \ll \xi$ . If we use the dynamic scaling hypothesis to match this behavior onto the characteristic frequency  $\bar{\omega}_{\xi^{-1}}$ , at  $k = \xi^{-1}$ , we find that the diffusion constant  $D_m$  diverges, for  $T \rightarrow 0$ ,

$$D_m \sim T^{1/2} \xi / (\chi_{\perp}^0)^{1/2}. \quad (4.21)$$

### V. APPLICATION TO SPIN- $\frac{1}{2}$ ANTIFERROMAGNETS

#### A. Correlation length in the renormalized classical regime

In Sec. III we have demonstrated that, at least to one-loop order, the QNL $\sigma$ M maps onto a classical problem with a renormalized spin stiffness  $\rho_s$  and a short-wavelength cutoff of order  $\hbar c/k_B T$ , provided that the quantum coupling constant  $g_0$  is less than its critical value, the temperature  $T$  is finite and not too large, and the length scale is sufficiently large (renormalized classical regime). It is clear physically that the identification of the classical model and the QNL $\sigma$ M in the renormalized classical regime must hold beyond a one-loop calculation, so it is natural in this regime to exploit all the results known for the classical model. In particular, we shall, in the present section, obtain correlation length for our model by combining a two-loop  $\beta$ -function calculation with the available numerical simulations for the classical Heisenberg model on a two-dimensional lattice.

First, given the  $O(n)$  QNL $\sigma$ M at finite temperature, we integrate out all quantum fluctuations to obtain an effective classical  $O(n)$  NL $\sigma$ M. The calculation is explicitly carried out in Appendix E. We find that the action for the effective classical problem is given by ( $|\hat{\mathbf{n}}| = 1$ )

$$S_{\text{cl}} = \frac{1}{2t_0} \int d^2x |\mathbf{v}\hat{\mathbf{n}}|^2. \quad (5.1)$$

The coupling constant  $t_0$  is determined by

$$\frac{1}{t_0} = \frac{1}{k_B T} \left[ \rho_s(0) + \frac{k_B T(n-2)}{2\pi} \ln \left( \frac{\Lambda \hbar c}{k_B T} \right) + O(T^2) \right], \quad (5.2)$$

where  $\Lambda^{-1}$  is the length scale at which  $t_0$  is defined, and  $\rho_s(0)$  is the spin stiffness at  $T=0$  which is renormalized from the bare value by quantum fluctuations. We shall see later that  $O(T^2)$  term in the square brackets of Eq. (5.2) does not affect our evaluation of the correlation length at low temperatures. In the present section we shall only explicitly consider the case of two spatial dimensions.

It is now immediately possible to take over the two-loop  $\beta$  function calculated by Brézin and Zinn-Justin.<sup>50</sup> It must, however, be kept in mind that the renormalization-group equations derived by them are for the renormalized dimensionless temperature (coupling constant). Their renormalization-group equations follow from the invariance of the bare theory under a change of the renormalization point (an arbitrary momentum scale which defines the renormalized theory) holding the bare parameters fixed. To be consistent with the momentum-shell recursion method employed elsewhere, in the present paper we shall consider the flow of the bare coupling constants with the change of the length scale holding the physical correlation length fixed. Following Creutz<sup>51</sup> it is easy to see that up to two loops,  $\beta$  functions calculated in either way are identical. Therefore, the flow of the bare coupling constant is given by

$$\frac{dt}{dl} = \beta_2 t^2 + \beta_3 t^3, \quad (5.3)$$

where  $\beta_2 = (n-2)/2\pi$ , and  $\beta_3 = (n-2)/(2\pi)^2$ , and  $e^l$  is the length rescaling factor. For the  $O(3)$  symmetric model,  $n=3$ . In fact, the  $\beta$  function for the  $O(n)$  symmetric model, within the minimal subtraction scheme, is known up to four loops.<sup>52</sup> It is easy to show that  $\beta_2$  and  $\beta_3$  are universal, i.e., they do not depend on the precise regularization scheme used.<sup>51</sup> This, however, is not true for terms beyond two loops. The technique that we use below to calculate the correlation length for our model is well known in the context of lattice gauge theory.<sup>53</sup> Since it is less known to condensed-matter physicists, we shall work it out in detail.

Equation (5.3) can easily be integrated to obtain

$$-\frac{1}{\beta_2 t(l)} - \frac{\beta_3}{\beta_2^2} \ln t(l) = l - l^*. \quad (5.4)$$

Here  $l^*$  is simply an integration constant. The terms higher order in  $t$ , neglected in Eq. (5.4), are of no consequence to the discussion that follows.  $l^*$  is now determined by setting  $l=0$  in Eq. (5.4), and recognizing that  $t(0) \equiv t_0$  is nothing but the bare coupling constant. Thus

$$l^* = \frac{1}{\beta_2 t_0} + \frac{\beta_3}{\beta_2^2} \ln t_0. \quad (5.5)$$

Since the NL $\sigma$ M in two-space dimensions, described by Eq. (5.1), has no intrinsic scale, from dimensional

analysis, the physical correlation length  $\xi$  is given by

$$\xi = \frac{C_\xi}{\Lambda} (t_0)^{\beta_3/\beta_2^2} e^{1/\beta_2 t_0}, \quad (5.6)$$

where  $C_\xi$  is a pure number which cannot be fixed from the low-temperature ( $\beta_2 t_0 \ll 1$ ) renormalization-group equations (higher loop corrections cannot help in this respect). It is important to note that  $C_\xi$  depends on the precise regularization scheme (i.e., the precise cutoff scheme) used in defining our field theory. This statement follows trivially from the fact that the terms beyond two loops are nonuniversal in the  $\beta$  function. However, once a cutoff scheme is specified,  $C_\xi$  is also uniquely specified. Moreover,  $C_\xi$  is a pure number, and does not depend on the coupling constant  $t_0$ . Thus, in order to complete our calculation of the correlation function, we must find a way to compute  $C_\xi$ . We now describe how this is to be done.

First note that one can invert Eq. (5.5) to obtain

$$\frac{1}{t_0} = \beta_2 l^* + \frac{\beta_3}{\beta_2} \ln[l^* + O(t_0)]. \quad (5.7)$$

This is an interesting equation. It is precisely of the form that a direct loopwise perturbation theory would yield for the dependence of the bare coupling constant with scale. To see this more clearly, we rewrite Eq. (5.7) using Eq. (5.6). Thus,

$$\frac{1}{t_0} = \beta_2 \ln(\Lambda \xi / C_\xi) + \frac{\beta_3}{\beta_2} \ln[\ln(\Lambda \xi / C_\xi) + O(t_0)], \quad (5.8)$$

and represents the fact that  $t_0$  decreases logarithmically with increasing  $\Lambda$ . Recall that we are holding  $\xi$  constant. Most importantly, note that only a one-loop calculation is necessary to define  $C_\xi$ —i.e., the two-loop correction does not redefine  $C_\xi$ . Now imagine that the same calculation is carried out with a different regularization scheme. This would yield instead of Eq. (5.8) the following:

$$\frac{1}{t'_0} = \beta_2 \ln(\Lambda \xi / C'_\xi) + \frac{\beta_3}{\beta_2} \ln[\ln(\Lambda \xi / C'_\xi) + O(t'_0)]. \quad (5.9)$$

From Eqs. (5.8) and (5.9), we obtain

$$\frac{1}{t_0} - \frac{1}{t'_0} = \beta_2 \ln(C'_\xi / C_\xi). \quad (5.10)$$

The next step in the calculation is to find a relation between  $t_0$  and  $t'_0$ . For this we need simply a one-loop perturbation theoretic calculation. We need to compute renormalized coupling  $t_R$  for the bare couplings  $t_0$  and  $t'_0$ , and demand  $t_R$  be identical (equivalent to holding physical  $\xi$  fixed), i.e.,

$$t_R = \frac{t_0}{Z_1} = \frac{t'_0}{Z'_1}. \quad (5.11)$$

The definition of the renormalization factors  $Z_1$  is the same as that of Brézin and Zinn-Justin.<sup>50</sup> Later we shall see that to one-loop order

$$Z_1 = 1 + B(\Lambda)t_0, \quad (5.12)$$

$$Z'_1 = 1 + B'(\Lambda)t'_0. \quad (5.13)$$

From Eqs. (5.11)–(5.13), we get

$$t_0 = t'_0 + [B(\Lambda) - B'(\Lambda)]t_0^2, \quad (5.14)$$

or equivalently,

$$t'_0 = t_0 - [B(\Lambda) - B'(\Lambda)]t_0^2. \quad (5.15)$$

It is not difficult to guess that the general forms of the  $B$ 's are given by [note that  $\Lambda(\partial/\partial\Lambda)t_R = 0$  must yield the  $\beta$  function]

$$B(\Lambda) = -\beta_2 \ln \Lambda + A, \quad (5.16)$$

$$B'(\Lambda) = -\beta_2 \ln \Lambda + A'. \quad (5.17)$$

Explicit calculations of  $B$ 's are given below. We therefore get

$$t'_0 = t_0 - (A - A')t_0^2. \quad (5.18)$$

Now substituting Eq. (5.18) in Eq. (5.10), we get

$$\frac{1}{t_0} - \frac{1}{t_0[1 - (A - A')t_0]} = \beta_2 \ln(C'_\xi / C_\xi). \quad (5.19)$$

Simplifying Eq. (5.19) we get

$$C'_\xi / C_\xi = e^{(A' - A)/\beta_2}. \quad (5.20)$$

Therefore, one-loop calculations of the finite parts to the counter term  $Z_1$  immediately yield a relation between the constants  $C'_\xi$  and  $C_\xi$ . If by some means we can compute  $C_\xi$  in some regularization scheme, only one-loop calculations are necessary to determine the constant in any other regularization scheme.

A more general version of the above conversion is now easy to obtain. Consider two theories in which not only the regularization schemes differ, but also the scales of definitions of  $t_0$  and  $t'_0$ . Let these scales be respectively  $\Lambda$  and  $\Lambda'$ . Then for the correlation length we would get

$$\begin{aligned} \xi &= \frac{C_\xi}{\Lambda} (t_0)^{\beta_3/\beta_2^2} e^{1/\beta_2 t_0} \\ &= \frac{C'_\xi}{\Lambda'} (t'_0)^{\beta_3/\beta_2^2} e^{1/\beta_2 t'_0}. \end{aligned} \quad (5.21)$$

Instead of Eq. (5.10) we would have

$$\frac{1}{t_0} - \frac{1}{t'_0} = \beta_2 \ln \left[ \frac{\Lambda C'_\xi}{\Lambda' C_\xi} \right]. \quad (5.22)$$

Similarly, Eq. (5.18) will be replaced by

$$t'_0 = t_0 - [(A - A') + \beta_2 \ln(\Lambda'/\Lambda)]t_0^2. \quad (5.23)$$

This will now lead to the equation

$$\frac{1}{t_0} - \frac{1}{t_0\{1 - [(A - A') + \beta_2 \ln(\Lambda'/\Lambda)]t_0\}} = \beta_2 \ln \left[ \frac{\Lambda C'_\xi}{\Lambda' C_\xi} \right]. \quad (5.24)$$

Once again, we get

$$\frac{C'_\xi}{C_\xi} = e^{(A' - A)/\beta_2}. \quad (5.25)$$

The conversion factor  $C'_\xi/C_\xi$  between the lattice regularization scheme and the Pauli-Villars regularization scheme for  $O(n)$  NL $\sigma$ M was given by Parisi.<sup>54</sup> In what follows we shall work out a closely related conversion factor. Since  $t_0$  defined in Eq. (5.2) was obtained by a sharp momentum cutoff scheme (cf. Appendix E), we need to calculate the correlation length using the same cutoff procedure. This cutoff scheme is also consistent with the discussion in Appendix C, as well as the remainder of the paper. From Eq. (5.6) we immediately get (recall that the  $\beta$  function up to two loops is universal)

$$\xi = \frac{C_\xi^{\text{mom}}}{\Lambda} (t_0)^{\beta_3/\beta_2^2} e^{1/\beta_2 t_0}, \quad (5.26)$$

where  $C_\xi^{\text{mom}}$  is a constant specific  $t_0$  the momentum cutoff scheme. Substituting for  $\beta_3$ ,  $\beta_2$ , and to from Eq. (5.2), we get

$$\xi = C_\xi^{\text{mom}} \left( \frac{\hbar c}{k_B T} \right) \left( \frac{k_B T}{\rho_s(0)} \right)^{1/(n-2)} \exp \left[ \frac{2\pi\rho_s(0)}{(n-2)k_B T} \right], \quad (5.27)$$

where we have neglected logarithmic corrections in the

$$\Gamma^L(\mathbf{k}, H) = \frac{1}{t_0} G_0^{-1}(\mathbf{k}) + \frac{(n-1)H}{2} \sum_{\mathbf{p}} G_0(\mathbf{p}) + \sum_{\mathbf{p}} \left[ G_0(\mathbf{p}) \left( \frac{2}{a^2} [2 - \cos a(p_x + k_x) - \cos a(p_y + k_y)] + H \right) - 1 \right], \quad (5.32)$$

where following Brézin and Zinn-Justin<sup>50</sup> we have introduced a magnetic field  $H$  as the infrared regulator. The lattice propagator  $G_0(\mathbf{p})$  is given by

$$G_0(\mathbf{p}) = \frac{1}{\frac{2}{a^2} (2 - \cos a p_x - \cos a p_y) + H}. \quad (5.33)$$

The renormalization factor  $Z_\Gamma^L$  is now easy to calculate (our definitions are the same as those of Brézin and Zinn Justin<sup>50</sup>), and we get

$$Z_\Gamma^L = 1 - \frac{t_0}{4\pi} \left[ (n-2) \ln \left( \frac{32}{Ha^2} \right) + \pi \right], \quad (5.34)$$

where we have used the facts that

$$\begin{aligned} \sum_{\mathbf{p}} G_0(\mathbf{p}) &= \frac{a^2}{(2\pi)^2} \int_{-\pi/a}^{\pi/a} dp_x \int_{-\pi/a}^{\pi/a} dp_y \frac{1}{H + \frac{2}{a^2} (2 - \cos p_x a - \cos p_y a)} = \frac{1}{2\pi(1 + Ha^2/4)} K \left( \frac{1}{1 + Ha^2/4} \right) \\ &\rightarrow \frac{1}{4\pi} \ln \left( \frac{32}{Ha^2} \right), \quad H \rightarrow 0 \end{aligned} \quad (5.35)$$

and

$$\sum_{\mathbf{p}} \cos a p_x G_0(\mathbf{p}) = \frac{1}{4\pi} \left[ \ln \left( \frac{32}{Ha^2} \right) - \pi \right], \quad H \rightarrow 0. \quad (5.36)$$

$K(x)$  in Eq. (5.35) is the complete elliptic integral of the first kind.

The one-particle irreducible part in the one-loop approximation for the momentum cutoff model is given by

$$\Gamma^{\text{mom}}(k, H) = \frac{1}{t_0} (k^2 + H) + \left[ \frac{(n-1)H}{2} + k^2 \right] \int_{\Lambda} \frac{d^2 q}{(2\pi)^2} \frac{1}{q^2 + H}. \quad (5.37)$$

prefactor. Specializing to the case  $n=3$ , we have

$$\xi = C_\xi^{\text{mom}} \left( \frac{\hbar c}{\rho_s(0)} \right) e^{2\pi\rho_s(0)/k_B T}. \quad (5.28)$$

$C_\xi^{\text{mom}}$  is thus left undetermined.

On the other hand, the classical Heisenberg model (three-component unit vector) on a square lattice provides  $O(3)$  invariant regularization of the  $O(3)$  NL $\sigma$ M. Instead of Eq. (5.26) we now get ( $a \equiv$  lattice spacing)

$$\xi = a C_\xi^L (t_0)^{\beta_3/\beta_2^2} e^{1/\beta_2 t_0}. \quad (5.29)$$

Since  $n=3$ , in this case,

$$\xi = a C_\xi^L t_0 e^{2\pi/t_0}. \quad (5.30)$$

Note that  $2\pi C_\xi^L \equiv B_\xi$  defined earlier in Sec. IV. Given the fact that we know  $C_\xi^L$  we can use Eq. (5.25) to calculate  $C_\xi^{\text{mom}}$ , i.e., use

$$\frac{2\pi C_\xi^{\text{mom}}}{2\pi C_\xi^L} = e^{(A^{\text{mom}} - A^L)\beta_2}. \quad (5.31)$$

To calculate  $A^{\text{mom}}$  and  $A^L$  we need to compute  $Z_\Gamma^{\text{mom}}$  and  $Z_\Gamma^L$ , respectively.  $Z_\Gamma^L$  was already calculated by Parisi.<sup>54</sup> We give here some details since his paper contains a number of printing errors.

The one-particle irreducible part  $\Gamma$  for the lattice model can be written in one-loop approximation as

The loop integral is now given by

$$\int_{\Lambda} \frac{d^2q}{(2\pi)^2} \frac{1}{q^2+H} = \frac{1}{2\pi} \int_0^{\Lambda} dq \frac{q}{q^2+H} \rightarrow \frac{1}{4\pi} \ln \left[ \frac{\Lambda^2}{H} \right], \quad H \rightarrow 0. \quad (5.38)$$

A simple calculation then yields

$$Z_1^{\text{mom}} = 1 - \frac{t_0}{4\pi} (n-2) \ln \left[ \frac{\Lambda^2}{H} \right]. \quad (5.39)$$

From Eqs. (5.34) and (5.39) we get

$$A^{\text{mom}} = -\beta_2 \ln \frac{1}{\sqrt{H}}, \quad (5.40)$$

and

$$A^L = -\beta_2 \left[ \frac{\pi}{2(n-2)} + \ln \left( \frac{32}{H} \right)^{1/2} \right]. \quad (5.41)$$

Therefore, we get from Eq. (5.31)

$$C_{\xi}^{\text{mom}} = C_{\xi}^L \sqrt{32} e^{\pi/2(n-2)}. \quad (5.42)$$

For  $n=3$

$$C_{\xi}^{\text{mom}} = C_{\xi}^L \sqrt{32} e^{\pi/2} \approx 27.2 C_{\xi}^L. \quad (5.43)$$

Combining Eqs. (5.28) and (5.43) we get, finally, for our QNL $\sigma$ M, in the renormalized classical regime,

$$\xi = \sqrt{32} e^{\pi/2} (2\pi C_{\xi}^L) \left( \frac{\hbar c}{2\pi\rho_s(0)} \right) \exp \left( \frac{2\pi\rho_s(0)}{k_B T} \right). \quad (5.44)$$

As mentioned earlier in Sec. IV,  $2\pi C_{\xi}^L$  ranges between 0.01 and 0.013, with a quoted uncertainty of the order of 30%; the quantities  $\rho_s(0)$  and  $c$  are the spin-stiffness constant and spin-wave velocity of the quantum antiferromagnet at long wavelengths and  $T=0$ .

It is to be noted that the uncertainty in the prefactor in the one-loop approach, as discussed in Sec. III, is now completely eliminated.

#### B. $\rho_s$ and $\chi_{\perp}$ for the two-dimensional $S = \frac{1}{2}$ antiferromagnet

We use spin-wave theory to calculate  $\rho_s(0)$  ( $\equiv \rho_s$ ) appearing in Eq. (5.44). We know from the work of Ogu-chi<sup>16</sup> that for the spin- $S$  antiferromagnet on a square lattice with lattice constant  $a$  and nearest-neighbor exchange constant  $J$ , at  $T=0$ ,

$$\chi_{\perp}(0) = \frac{\hbar^2}{8Ja^2} Z_x(S) \quad (5.45)$$

and

$$c = \frac{\sqrt{8}Jsa}{\hbar} Z_c(S), \quad (5.46)$$

where the correction factors are given by

$$Z_x = 1 - 0.552/2S + O(1/2S)^2 \quad (5.47)$$

and

$$Z_c = 1 + 0.158/2S + O(1/2S)^2. \quad (5.48)$$

$O(1/2S)^2$  terms in  $Z_x$  and  $Z_c$  are expected to be small if the system is well into the ordered phase at  $T=0$ . For  $S = \frac{1}{2}$  we get  $Z_x = 0.448$ , if we ignore the correction terms in (5.47). It is interesting to compare this value with that obtained by Lines<sup>55</sup> using random-phase approximation which is 0.523. Using the relation  $\rho_s = c^2 \chi_{\perp}(0)$ , we can write

$$\rho_s = JS^2 Z_c^2(S) Z_x(S) \equiv JS^2 Z_{\rho_s}(S). \quad (5.49)$$

For  $S = \frac{1}{2}$  we get, using (5.47) and (5.48),

$$\rho_s \approx 0.15J. \quad (5.50)$$

Alternately, we can also write

$$2\pi\rho_s = C_{\rho_s} \left( \frac{\hbar c}{a} \right), \quad (5.51)$$

where  $C_{\rho_s} = 2\pi S Z_x Z_c / \sqrt{8}$ . For  $S = \frac{1}{2}$ ,  $C_{\rho_s} \approx 0.576$ . Finally, the expression (5.44) for the correlation length can be written for the 2D  $S = \frac{1}{2}$  AF as

$$\xi = C_{\xi} a e^{2\pi\rho_s/k_B T}, \quad (5.52)$$

where  $C_{\xi} \approx 0.5$  and  $2\pi\rho_s$  is given by Eq. (5.51) with  $C_{\rho_s} \approx 0.576$ .

Equation (4.8) for  $S(k=0)$  can now be applied directly to the quantum antiferromagnet. One obtains

$$S(k=0) \sim C_s a^2 \left( \frac{k_B T}{2\pi\rho_s} \right)^2 e^{4\pi\rho_s/k_B T} \quad (5.53)$$

where

$$C_s = B_s C_{\xi}^2 N_0^2. \quad (5.54)$$

The results of spin-wave calculations and other analyses of the  $S = \frac{1}{2}$  antiferromagnet give<sup>9</sup>  $N_0 \approx 0.31$ , in units where the fully aligned Néel state would have  $N_0 = \frac{1}{2}$ . [Note that for  $k_B T \gg J$ , one has  $S(k) = 3a^2/4$ , with our definitions.] Combined with our previous estimates this gives

$$C_s \approx 4.3. \quad (5.55)$$

The results of Sec. IV for the dynamics of the classical lattice rotator model can also be applied to the quantum antiferromagnet. As for the static problem, we identify  $\rho_s^0$  of the CLRM with the zero-temperature spin stiffness  $\rho_s$  of the antiferromagnet,  $\chi_{\perp}^0$  is identified with the zero temperature  $\chi_{\perp}(0)$  of the antiferromagnet, and the lattice constant  $b$  is a constant times thermal wavelength ( $\hbar c/k_B T$ ). Dynamic results which were expressed in terms of the product  $(k\xi)$ , without explicit reference to other parameters, can of course be carried over directly.

The result (4.15) for the characteristic frequency at  $k=0$ , becomes in the quantum system

$$\bar{\omega}_0 \sim \text{const} \left( \frac{k_B T}{2\pi\rho_s} \right)^{1/2} \xi^{-1} c \quad (5.56)$$

in the limit where  $\xi \rightarrow \infty$ .

The dynamic scaling function  $\Phi(x, y)$ , which appears in Eq. (4.13), should be the same for the quantum antiferromagnet and the CLRM. Since this function is not known at present, however, it may be helpful to guess a simple form, with several adjustable parameters, which then may be fit to experimental data. One such form, consistent with the dynamic scaling hypothesis, is

$$S(k, \omega) = S(k) \operatorname{Im} \left[ \frac{1}{\omega - \alpha_k - i\theta} + \frac{1}{\omega + \alpha_k - i\theta} \right], \quad (5.57)$$

where  $\theta$  is chosen to be a constant times  $\bar{\omega}_0$ , independent of  $k$ , and

$$\alpha_k \equiv \left(\frac{3}{2}\right)^{1/2} [1 + \frac{1}{2} \ln(1 + k^2 \xi^2)]^{1/2} \times (k^2 + \delta \xi^{-2})^{1/2} \left[ \frac{k_B T}{2\pi\rho_s} \right]^{1/2} c, \quad (5.58)$$

where  $\delta$  is a second adjustable parameter, introduced to permit a non-Lorentzian line shape for  $k=0$ . A better approximation would allow the damping  $\theta$  to depend on  $k$  in such a manner that the spin-wave width can increase with increasing  $k$ , as discussed in Sec. IV. Note that for large values of  $k\xi$ , the position of the spin-wave peak  $\alpha_k$  contains no adjustable parameters, in the limit of small  $k_B T/2\pi\rho_s$ , assuming that the zero-temperature parameters  $\rho_s$  and  $c$  are known.

It is possible to compare our results with those obtained by Manousakis and Salvador<sup>56</sup> from a Monte Carlo simulation of a  $S = \frac{1}{2}$  nearest-neighbor Heisenberg model on a square lattice. Since our expression for  $\xi$  should be valid when  $2\pi\rho_s/k_B T \gg 1$ , we compare the results obtained by them at their lowest temperature  $T/J=0.4$ . For this purpose we write Eq. (5.52) as ( $S = \frac{1}{2}$ )

$$\xi/a = C_\xi e^{0.94J/T}. \quad (5.59)$$

We find for  $T/J=0.4$ ,  $\xi/a=4.9$  instead of 13 as found by them. In spite of the uncertainties in  $C_\xi$ , the difference seems difficult to reconcile. By contrast, at  $T/J=0.5$  we get  $\xi/a=3.1$  which is close to the value 3.4 obtained by Manousakis and Salvador<sup>56</sup> at that temperature. Thus, the discrepancy might be explained if they have overestimated the increase in  $\xi$  between the temperatures  $T/J=0.5$  and  $T/J=0.4$ .

In principle, one might also compare Eq. (5.53) for  $S(k=0)$  with results from Monte Carlo simulations of the  $S = \frac{1}{2}$  antiferromagnet. However, a serious problem arises because the value of  $k_B T/2\pi\rho_s$  is only of order  $\frac{1}{2}$  in these simulations. The renormalization-group analysis employed by Shenker and Tobochnik suggests that for moderate temperatures it may be a better approximation to replace  $t_0$  by  $t_0/(1+t_0/2\pi)$  in the preexponential factors of (4.5) and (4.8a). In this spirit, one should then replace (5.52) and (5.53) by

$$\xi \approx \frac{C_\xi a e^{2\pi\rho_s/k_B T}}{1 + (k_B T/2\pi\rho_s)}, \quad (5.60)$$

$$S(k) \approx \frac{C_s a^2 (k_B T/2\pi\rho_s)^2 e^{4\pi\rho_s/k_B T}}{[1 + (k_B T/2\pi\rho_s)]^4}. \quad (5.61)$$

The correction to  $S(k)$  is particularly large.

## VI. COMPARISON WITH EXPERIMENTS IN $\text{La}_2\text{CuO}_4$

The experimental dependence of the correlation length  $\xi$  obtained in Ref. 4 as a function of temperature is shown in Fig. 4. The data plotted here are for their "best sample," i.e., the sample with highest Néel temperature  $T_N=195$  K. In our earlier paper<sup>5</sup> we attempted to fit the data with the one-loop result given in Sec. III. In this approach, well within the renormalized classical regime, one can write

$$\xi = 0.9 \left[ \frac{\hbar c}{k_B T} \right] \exp(2\pi\rho_s/k_B T), \quad (6.1)$$

where  $2\pi\rho_s = C_{\rho_s}(\hbar c/a)$  with  $C_{\rho_s} \cong 0.576$  as shown previously. The preexponential factor in the one-loop approximation cannot be reliable. Nonetheless, we obtained an excellent fit with  $\hbar c = 0.425$  eV Å.

One of the major emphases of the present paper has been to show that this preexponential factor in the renormalized classical regime can be fixed unambiguously if one combines classical Monte Carlo simulation results with the two-loop calculation. This was discussed extensively in Sec. V. None of the uncertainties encountered in the one-loop approach appear anymore. We now obtain for  $\xi$  the expression

$$\xi = C_\xi a \exp(2\pi\rho_s/k_B T), \quad (6.2)$$

where the lattice constant  $a$  is 3.8 Å and  $C_\xi \approx 0.5$ . The uncertainties in the classical simulation may lead to as large as 30% uncertainty in  $C_\xi$ . With a better simulation of the classical problem it may be possible to determine  $C_\xi$  more accurately. Moreover, there may be of the order of 10%–15% uncertainty in the spin-wave approximations at  $T=0$  that we have used to determine  $Z_{\rho_s}$ . This, in turn, would lead to additional 10%–15% error in  $C_\xi$  as well as 10%–15% error in  $\rho_s$ . Furthermore, one must bear in mind that the formula (6.2) is valid asymptotically, i.e.,

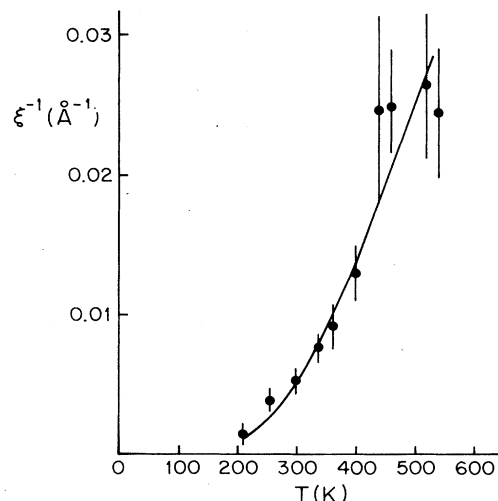


FIG. 4. Inverse correlation length  $\xi^{-1}$  as a function of temperature  $T$ . The data are taken from Ref. 4. The solid line is the fit  $\xi/a = A \exp(B/T)$ , where  $A=1$ , and  $B=1175$  K.

for  $2\pi\rho_s/k_B T \gg 1$ .

The data can be fit very well with the formula (6.2) with  $2\pi\rho_s = 1175$  K and  $C_\xi = 1$ . This implies  $\hbar c = 0.66$  eV Å using Eq. (5.51). The fit shown in Fig. 4 is nearly identical to that obtained with the one-loop formula (6.1) and  $\hbar c = 0.425$  eV Å. The value  $C_\xi = 1$  should be compared to the theoretical value  $C_\xi \approx 0.5$  that we obtained in Sec. V. Given the uncertainties discussed earlier *and* the uncertainties in the experimental data we find the results to be extremely reasonable. Note that  $\hbar c = 0.66$  eV Å corresponds to  $J \approx 1200$  K.

The experimental data cannot, however, be fit if we assume that the  $T=0$  state is disordered, as was pointed out earlier.<sup>5</sup> For example, if  $\bar{g}_0 = 1$  we have argued that, quite generally,  $\xi^{-1} = k_B T / C_Q \hbar c$ , where  $C_Q$  is a universal number of the order of unity. From the experimental data shown in Fig. 3 such a linear temperature dependence of  $\xi^{-1}$  passing through the origin can be immediately ruled out. If our scenario of the quantum disordered phase is correct it would be even harder to fit the data with  $\bar{g}_0 > 1$ .

It is natural to ask how our theory does with respect to other known experimental facts. Since we have assumed the validity of spin-wave theory at  $T=0$  we would predict a staggered magnetization of  $0.6\mu_B$  per site at  $T=0$ . Recent quantum Monte Carlo simulations (see Reger and Young, and Gross, Sánchez-Velasco, and Siggia in Ref. 9) seem to find a staggered magnetization rather close to the spin-wave result. Similar conclusions were also reached by Huse<sup>9(b)</sup> and Shankar and Murthy.<sup>9(d)</sup> Experimental results for the staggered magnetization vary. The largest staggered magnetization observed<sup>57</sup> so far in  $\text{La}_2\text{CuO}_4$  is  $0.5\mu_B$ , while for the sample for which the correlation length data is shown in Fig. 4, the  $T=0$  staggered magnetization is  $0.35\mu_B$ .

Because the Néel temperature of  $\text{La}_2\text{CuO}_4$  is extremely sensitive to impurities and defects (e.g., oxygen vacancies), it might be incorrect to ignore the effects of impurities even in the best samples which have been studied so far. Quenched impurities become defect rods in the time-like direction of the QNL $\sigma$ M which destroys the Lorentz invariance of the model. We expect that at the quantum transition point there will be new critical exponents dominated by randomness.<sup>58</sup> Recently some progress has been made in understanding the role of quenched impurities well into the ordered phase.<sup>59</sup> By means of a renormalization-group analysis it has been shown that for small randomness random couplings are irrelevant, but random fields are relevant for the long-distance properties of the quantum antiferromagnetic ground state in two dimensions.

The experiments also show a transition to three-dimensional Néel order at  $T_N = 195$  K, which is quite likely to be triggered by a weak exchange coupling  $J'$  between the  $\text{CuO}_2$  planes. The transition should occur when  $J'(N_0/S)^2(\xi/a)^2 \approx k_B T_N$ , where  $N_0/S$  is the reduction in the  $T=0$  staggered magnetization relative to the Néel value induced by 2D quantum fluctuations. Using  $\xi(T_N) \approx 200a$  from experiments and  $(N_0/S)^2 \approx 0.36$  we find  $J'$  to be  $0.015$  K as compared to  $J \approx 1200$  K, i.e.,  $J' \sim 10^{-3}J$ . A simple mean-field treatment of weakly coupled planes of quantum spins, as discussed in Appen-

dix F, shows that such a small value of  $J'$  has a negligible effect on our estimates for  $\rho_s$ ,  $\chi_\perp$ , and  $N_0/S$  at  $T=0$ . Such a small  $J'$  has also very little effect on the 2D fluctuations seen above  $T_N$ . For transitions which are driven by small interplanar interactions, coupling large two-dimensionally correlated regions (in the present case the linear dimension of such a region is of the order of  $200a$ ), the critical region may be expected to be rather narrow.

In contrast, if we had assumed  $\bar{g}_0 \geq 1$ , so that the isolated layer has  $N_0=0$ , then it would be necessary to choose a very large value of  $J'$ , comparable to  $J$ , in order to account for the actual staggered magnetization observed in  $\text{La}_2\text{CuO}_4$ . Scaling predicts that  $N_0/S \propto (J'/J)^{(1+\eta_3)/(4-2\eta_3)}$ , for  $\bar{g}_0 = 1$ . Here,  $\eta_3$  is the familiar critical exponent for the 3D Heisenberg model. A large value of  $J'$  would be inconsistent with the fact that the observed spin-correlations are two dimensional for  $T > T_N$ . Similar inconsistencies arise if one assumes that the observed magnetization is due to perturbations which break the spin isotropy of the Heisenberg Hamiltonian.

In Sec. IV we have elaborated on our predictions for the dynamics of the system based on dynamic scaling hypothesis. Presumably, with better experiments it would be possible to test these predictions. For  $k\xi \ll 1$ , theory predicts a quasielastic peak of a few meV width at 300 K. The failure to observe a quasielastic peak in experiments so far may indicate a disagreement with our theory.

## VII. CONCLUSION

Motivated by recent experiments on  $\text{La}_2\text{CuO}_4$  we have examined the low-temperature properties of two-dimensional quantum antiferromagnets. In what follows, we briefly summarize the main points which we tried to make in our paper.

(1) The low-temperature properties of the two-dimensional  $S = \frac{1}{2}$  nearest-neighbor Heisenberg model can be well described by the quantum-mechanical nonlinear  $\sigma$  model. Such a model is the simplest continuum model one can think of which has the correct symmetry, the correct spin-wave spectrum, and the correct interaction between spin waves at long wavelengths. This model also has a quantum disordered phase which bears some resemblance to the various hypothetical states that have been described as RVB states.

(2) It is at least a reasonable hypothesis that the ordered phase of the QNL $\sigma$ M has identical properties to the ordered phase of 2D  $S = \frac{1}{2}$  AF. It is more questionable, however, whether the disordered phase is an accurate description of the disordered phases of quantum antiferromagnets (which may exist for 2D antiferromagnets with frustrating interactions, even if it does not exist for the nearest-neighbor square lattice case). Indeed, in 1D we believe that there are differences between the cases of the integer and the half-integer spin which require at least an extension of the QNL $\sigma$ M in the half-integer case. Nevertheless, it seems most worthwhile to explore the consequences of QNL $\sigma$ M as it stands.

(3) Spin-wave calculations and other theoretical work predict that the system is ordered at  $T=0$ . However, at

finite temperatures there will necessarily be a finite correlation length. These features are shared by the QNL $\sigma$ M in the appropriate range of coupling constants.

(4) The one-loop approximation should be qualitatively correct but not quantitative in the quantum regime, which corresponds to the  $(d+1)$ -dimensional classical model. However, the scaling result that  $\xi = C_Q \hbar c / k_B T$  for  $\bar{g}_0 = 1$ , and the statement that  $\xi < C_Q \hbar c / k_B T$  for  $\bar{g}_0 > 1$ , should be correct even for a proper calculation of the model.

(5) A calculation to two-loop order gives a correct description of the classical 2D Heisenberg model at low temperatures. The two-loop correction only affects the preexponential factor for the correlation length. A similar correction for the renormalized classical regime was obtained in the present paper. This is the regime of greatest interest for the actual experiments. The correlation lengths obtained in neutron scattering can be fit quite well by our theory with very reasonable choices of spin-wave velocity and coupling constant. It seems difficult, however, to fit the data with this model if the coupling constant is in the range where there is no order at  $T=0$ .

(6) The combination of the large observed correlation lengths in the temperature-disordered phase of  $\text{La}_2\text{CuO}_4$ , and the two dimensionality of the scattering, make it seem very unlikely that the observed staggered magnetization in the 3D ordered phase could only be the result of interlayer coupling or anisotropy.

(7) The evidence so far seems most consistent with the assumption that the 2D  $S = \frac{1}{2}$  nearest-neighbor Heisenberg antiferromagnet on a square lattice has order at  $T=0$ .

(8) Based on dynamic scaling hypothesis we have also made predictions of the dynamics of the system which can be tested in the future with more precise and refined experiments.

#### ACKNOWLEDGMENTS

This work was supported in part by the National Science Foundation through Grants No. DMR-86-01908 (S.C.) and No. DMR-85-14638 (B.I.H. and D.R.N.), and in part by the Harvard Materials Research Laboratory. We would like to thank P. W. Anderson, R. J. Birgeneau, P. A. Fleury, G. Gomez-Santos, E. Manousakis, G. Shirane, and S. Tyc for useful discussions. S.C. would also like to thank the Harvard Physics Department and the Materials Research Laboratory for their hospitality during a visit.

#### APPENDIX A: SUBLATTICE MAGNETIZATION OF $S = \frac{1}{2}$ AF ON A SQUARE LATTICE WITH NEXT-NEAREST-NEIGHBOR ANTIFERROMAGNETIC INTERACTION

Let us rewrite the Hamiltonian (1.1) in the following form:

$$\mathcal{H} = J \sum_{\langle j,l \rangle} \mathbf{S}_j \cdot \mathbf{S}_l + J'' \sum_{\langle j,j' \rangle} \mathbf{S}_j \cdot \mathbf{S}_{j'} + J''' \sum_{\langle l,l' \rangle} \mathbf{S}_l \cdot \mathbf{S}_{l'} + h_1 \sum_j S_j^z + h_2 \sum_l S_l^z, \quad (\text{A1})$$

where the sites  $\{j, j'\} \in A$  and the sites  $\{l, l'\} \in B$ .  $h_1$  and  $h_2$  are the magnetic fields acting on the two sublattices. Introducing Holstein-Primakoff transformation<sup>43</sup> given by

$$S_j^+ = \sqrt{2S} f_j(S) a_j, \quad S_l^+ = \sqrt{2S} b_l^+ f_l(S), \quad (\text{A2})$$

$$S_j^z = S - a_j^+ a_j, \quad S_l^z = -S + b_l^+ b_l,$$

where  $f_j(S) = (1 - n_j/2S)^{1/2}$  [similarly for  $f_l(S)$ ], we now expand  $\mathcal{H}$  in powers of  $1/S$ . A straightforward calculation then leads to an expression for the ground-state energy. A derivative of the energy with respect  $h_1$  then leads to the sublattice magnetization given by ( $h_1 \rightarrow 0$ ,  $h_2 \rightarrow 0$ ):

$$\langle S_z \rangle_A = \frac{NS}{2} \left[ 1 + \frac{1}{S} \left( \frac{1}{2} - \frac{1}{N} \sum_k \frac{a_k}{\sqrt{a_k^2 - \gamma_k^2}} \right) - \frac{1}{S^2} \left( \frac{J''}{J} \right) \left( \frac{1}{N} \sum_k \frac{\gamma_k^2 (1 - \Gamma_k)}{(a_k^2 - \gamma_k^2)^{3/2}} \right) \left( \frac{1}{N} \sum_k \frac{a_k \Gamma_k - \gamma_k^2}{\sqrt{a_k^2 - \gamma_k^2}} \right) \right], \quad (\text{A3})$$

where

$$a_k = 1 - \frac{J''}{J} (1 - \Gamma_k). \quad (\text{A4})$$

$\Gamma_k$  and  $\gamma_k$  are given by

$$\Gamma_k = \frac{1}{4} \sum_{\delta'} e^{i\mathbf{k} \cdot \delta'} \quad (\text{A5})$$

and

$$\gamma_k = \frac{1}{4} \sum_{\delta} e^{i\mathbf{k} \cdot \delta}. \quad (\text{A6})$$

Here  $\delta'$  are nearest-neighbor lattice vectors on the sublattices  $A$  or  $B$ ;  $\delta$  are the nearest-neighbor lattice vectors on the original square lattice.

As discussed in Sec. I, the expansion (A3) can be ex-

pressed in terms of the coefficients

$$\alpha(J''/J) = -\frac{1}{2} + \frac{1}{N} \sum_k \frac{a_k}{\sqrt{a_k^2 - \gamma_k^2}}, \quad (\text{A7})$$

$$I_1 = \frac{1}{N} \sum_k \frac{\gamma_k^2 (1 - \Gamma_k)}{(a_k^2 - \gamma_k^2)^{3/2}}, \quad (\text{A8})$$

$$I_2 = -\sum_k \frac{a_k \Gamma_k - \gamma_k^2}{\sqrt{a_k^2 - \gamma_k^2}}, \quad (\text{A9})$$

which are tabulated numerically for a variety of values of  $J''/J$  in Table I.

Numerical evaluation suggests that  $\langle S_z \rangle_A$  can be made to vanish by increasing the ratio  $(J''/J)$ . The results are shown in Fig. 1. It does not of course follow that the state reached by varying  $J''/J$  is necessarily a quantum disordered state, e.g., the state reached may be an antifer-

TABLE I.  $a(J''/J)$ ,  $I_1(J''/J)$ , and  $I_2(J''/J)$  as a function of  $J''/J$ .

$J''/J$	$a(J''/J)$	$I_1(J''/J)$	$I_2(J''/J)$
0.00	0.196	0.581	0.260
0.05	0.212	0.686	0.271
0.10	0.231	0.826	0.283
0.15	0.253	1.02	0.297
0.20	0.282	1.29	0.314
0.25	0.319	1.69	0.334
0.30	0.369	2.36	0.361
0.35	0.441	3.57	0.397
0.40	0.559	6.29	0.451
0.45	0.805	15.9	0.554

romagnet with a vector in the [10] direction rather than the [11] direction.

#### APPENDIX B: HAMILTONIAN FORMULATION OF THE QUANTUM NONLINEAR $\sigma$ MODEL

To see how Eq. (2.9) follows from (2.8) in detail it will be useful to first soften the fixed-length constraint and work with variables of arbitrary length, namely

$$\mathbf{r}_i \equiv r_i \hat{\mathbf{n}}_i \quad (\text{B1})$$

with Lagrangian

$$\begin{aligned} \mathcal{L}(\{\mathbf{r}_i\}, \{\dot{\mathbf{r}}_i\}) = & \frac{1}{2} m \sum_i \left| \frac{d\mathbf{r}_i(t)}{dt} \right|^2 \\ & - \frac{1}{2} K \sum_{\langle i,j \rangle} |\mathbf{r}_i - \mathbf{r}_j|^2 - \sum_i U(r_i). \end{aligned} \quad (\text{B2a})$$

Here, the notation is intended to suggest “particles” with mass  $m$  and displacements  $\{\mathbf{r}_i\}$  connected by Hookean springs with spring constant  $K$ . Each particle also sits in a potential well,

$$U(\mathbf{r}) = \lambda [|\mathbf{r}|^2 - 1]^2, \quad (\text{B2b})$$

and we shall ultimately be interested in taking the limit of large  $\lambda$ . When  $\lambda \rightarrow \infty$ , Eq. (B2b) reduces to Eq. (2.8) with the identifications

$$m = b^d \rho_s^0 / c_0^2 = b^d \chi_{\perp}^0, \quad (\text{B3a})$$

$$K = b^{d-2} \rho_s^0. \quad (\text{B3b})$$

With constraint of fixed lengths relaxed, we can proceed in the usual way<sup>60</sup> to define the canonically conjugate momentum

$$\mathbf{p}_i = \frac{\partial \mathcal{L}}{\partial \dot{\mathbf{r}}_i} = m \dot{\mathbf{r}}_i \quad (\text{B4})$$

and Hamiltonian

$$\begin{aligned} \mathcal{H} = & \sum_i \mathbf{p}_i \cdot \dot{\mathbf{r}}_i - \mathcal{L} \\ = & \sum_i \frac{|\mathbf{p}_i|^2}{2m} + \frac{1}{2} K \sum_{\langle i,j \rangle} |\mathbf{r}_i - \mathbf{r}_j|^2 + \sum_i U(r_i). \end{aligned} \quad (\text{B5})$$

The angular momentum associated with each lattice site is

$$\mathbf{M}_i = \mathbf{r}_i \times \mathbf{p}_i. \quad (\text{B6})$$

We now quantize (B5), by setting

$$\mathbf{p}_i = \frac{\hbar}{i} \frac{\partial}{\partial \mathbf{r}_i}. \quad (\text{B7})$$

Just as in treatments of diatomic molecules with separation  $r_i$ ,<sup>61</sup> we can separate the quantum mechanics associated with (B5) into a “vibrational” part, describing the radial degrees of freedom  $r_i$ , and a “rotational” part, associated with the  $\{\hat{\mathbf{n}}_i\}$ .

To carry out this separation formally, we write the kinetic-energy terms in (B5) as

$$|\mathbf{p}_i|^2 = \frac{|\mathbf{M}_i|^2}{r_i^2} + p_{r_i}^2, \quad (\text{B8})$$

where

$$p_{r_i}^2 = \left( -\hbar^2 \frac{1}{r_i^2} \frac{\partial}{\partial r_i} r_i^2 \frac{\partial}{\partial r_i} \right)$$

is the radial part of the momentum-squared operator. When  $\lambda \rightarrow \infty$ , the spacing between vibrational energy levels associated with  $p_{r_i}^2$  and  $U(r_i)$  becomes large and all  $r_i$  will be locked into the lowest harmonic-oscillator level with negligible fluctuations about  $|\mathbf{r}_i| = 1$ . In the limit the Hamiltonian becomes

$$\mathcal{H} = \sum_i \frac{|\mathbf{M}_i|^2}{2m} + \frac{1}{2} K \sum_{\langle i,j \rangle} |\hat{\mathbf{n}}_i - \hat{\mathbf{n}}_j|^2 + \text{const}, \quad (\text{B9})$$

where the constant is due to the energy of the lowest-lying radial levels. Upon recalling the identifications (B3), we are led immediately to Eq. (2.9).

#### APPENDIX C: ONE-LOOP RECURSION RELATIONS FOR QUANTUM-MECHANICAL NONLINEAR $\sigma$ MODEL AND THE RENORMALIZED SPIN STIFFNESS

We follow Nelson and Pelcovits<sup>22</sup> and use momentum-shell method to derive the recursion relations. To get a more general set of recursion relations than that given in the text, consider  $S_{\text{eff}}$  in which we add a magnetic field, i.e.,

$$\begin{aligned} S_{\text{eff}}/\hbar = & \frac{\rho_s^0}{2\hbar} \int_0^{\beta\hbar} d\tau \int d^d x \left[ |\nabla \hat{\mathbf{n}}|^2 + \frac{1}{c^2} \left| \frac{\partial \hat{\mathbf{n}}}{\partial \tau} \right|^2 \right] \\ & - \frac{H}{\hbar} \int_0^{\beta\hbar} d\tau \int d^d x \sigma(x, \tau) \end{aligned} \quad (\text{C1})$$

where we have defined the vector  $\hat{\mathbf{n}} \equiv \{\boldsymbol{\pi}, \sigma\}$ ;  $\boldsymbol{\pi}$  is a  $(n-1)$ -component vector. For the O(3) model  $n=3$ . Note that  $H$  has the dimension of energy. It is understood that the space integrals are cut off at short distances by a wave-vector cutoff  $\Lambda$ .

The partition function  $Z$  is given by

$$\begin{aligned}
Z &= \int \mathcal{D}\sigma(x, \tau) \int \mathcal{D}\pi(x, \tau) \prod_{x, \tau} \delta[\sigma^2(x, \tau) + \pi^2(x, \tau) - 1] e^{-S_{\text{eff}}/\hbar} \\
&= \int \mathcal{D}\pi(x, \tau) \prod_{x, \tau} \frac{1}{\sqrt{1 - \pi^2(x, \tau)}} \exp \left[ -\frac{1}{2g_0} \int_0^u dx_0 \int d^d x \left[ (\partial_\mu \pi)^2 + \frac{(\pi \cdot \partial_\mu \pi)^2}{(1 - \pi^2)} \right] \right] \exp \left[ \hbar \int_0^u dx_0 \int d^d x \sqrt{1 - \pi^2} \right],
\end{aligned} \tag{C2}$$

where

$$g_0 = \frac{\hbar c}{\rho_s^0} \Lambda^{d-1}, \tag{C3}$$

$$h = \frac{H \Lambda^{-(1+d)}}{\hbar c}, \tag{C4}$$

and

$$u = \beta \hbar c \Lambda. \tag{C5}$$

Now  $x_0$  and  $\mathbf{x}$  are defined to be dimensionless variables, and  $\partial_\mu \equiv (\partial_0, \partial_1, \dots, \partial_d)$  are the derivatives with respect to these variables, and the wave-vector cutoff in (C2) is unity.

To proceed further we expand the factors  $(1 - \pi^2)^{-1}$  and  $\sqrt{1 - \pi^2}$  in Eq. (C2). We then expand  $\pi$ 's as

$$\pi(x_0, \mathbf{x}) = \sum_{n=-\infty}^{+\infty} \int \frac{d^d k}{(2\pi)^d} \pi(\omega_n, \mathbf{k}) e^{i\omega_n x_0 + i\mathbf{k} \cdot \mathbf{x}}, \tag{C6}$$

where the Matsubara frequencies  $\omega_n$  are  $2\pi n/u$  ( $n=0, \pm 1, \pm 2, \dots$ ). We now break up the  $\pi$  fields as follows:

$$\pi(\omega_n, \mathbf{q}) \equiv \begin{cases} \pi_{<}(\omega_n, \mathbf{q}), & 0 < |\mathbf{q}| < e^{-l}, \\ \pi_{>}(\omega_n, \mathbf{q}), & e^{-l} < |\mathbf{q}| < 1, \end{cases} \tag{C7}$$

and integrate out  $\pi_{>}$ , thereby generating an effective action involving only  $\pi_{<}$ . The  $q$ 's are then rescaled so that their range is restored to  $0 < |\mathbf{q}| \leq 1$ . The  $\pi_{<}$ 's are also rescaled, by the spin rescaling factor  $\zeta$ . The procedure is identical to that given by Nelson and Pelcovits<sup>22</sup> and we obtain

$$u' = u e^{-l}, \tag{C8}$$

$$\left( \frac{u}{g_0} \right)' = \zeta^2 e^{-(d+2)l} \left( \frac{u}{g_0} + I_{\text{loop}} \right), \tag{C9}$$

$$(hu)' = \zeta^2 e^{-dl} [hu + \frac{1}{2} hg_0(n-1)I_{\text{loop}}]. \tag{C10}$$

The spin rescaling factor  $\zeta$  can be easily determined by noting that  $hu$  must scale trivially, i.e.,  $(hu)' = \zeta(hu)$ .<sup>22</sup> Thus, we get

$$\zeta = e^{dl} \left[ 1 - \frac{g_0}{2u} (n-1)I_{\text{loop}} \right]. \tag{C11}$$

The loop integral  $I_{\text{loop}}$  is given by

$$\begin{aligned}
I_{\text{loop}} &= \sum_{n=-\infty}^{+\infty} \int \frac{d^d k}{(2\pi)^d} \frac{1}{k^2 + \omega_n^2 + hg_0} \\
&= \frac{K_d u}{2} \int_{e^{-l}}^1 dk \frac{k^{d-1}}{\sqrt{k^2 + hg_0}} \coth \left[ \frac{u}{2} \sqrt{k^2 + hg_0} \right]
\end{aligned} \tag{C12}$$

where  $K_d^{-1} = 2^{d-1} \pi^{(d/2)} \Gamma(d/2)$ . If we define  $\tilde{h} = hg$ , then we get from Eqs. (C8)-(C11)

$$\frac{dg}{dl} = (1-d)g + \frac{1}{2} K_d (n-2) g^2 \frac{1}{\sqrt{1+\tilde{h}}} \coth \left[ \frac{g}{2t} \sqrt{1+\tilde{h}} \right], \tag{C13}$$

$$\frac{dt}{dl} = (2-d)t + \frac{1}{2} K_d (n-2) g t \frac{1}{\sqrt{1+\tilde{h}}} \coth \left[ \frac{g}{2t} \sqrt{1+\tilde{h}} \right], \tag{C14}$$

$$\frac{d\tilde{h}}{dl} = 2\tilde{h} + \frac{1}{2} K_d (n-3) \tilde{h} g \frac{1}{\sqrt{1+\tilde{h}}} \coth \left[ \frac{g}{2t} \sqrt{1+\tilde{h}} \right], \tag{C15}$$

where we have defined  $t = k_B T \Lambda^{d-2} / \rho_s$ . Note that the dimensionless slab thickness in the imaginary time direction is  $u = \beta \hbar c \Lambda = g/t$ , and hence scales trivially as given in Eq. (C8). If we set  $H=0$  we obtain the recursion relations given in Sec. III.

We can use these recursion relations to calculate the renormalized spin stiffness  $\rho_s$  at  $T=0$  when  $d=2$  and  $n=3$ . We shall need Eq. (C13) in this limit, which reads

$$\frac{dg}{dl} = -g + \frac{g^2}{4\pi}. \tag{C16}$$

Because  $\rho_s$  defines a correlation length  $\xi_J$  in the Néel phase for  $g < g_c$  via the Josephson relation<sup>36</sup>

$$\xi_J = \frac{\hbar c}{\rho_s}, \tag{C17}$$

and because  $c$  is unrenormalized, the spin stiffness satisfies the simple renormalization-group scaling equation

$$\rho_s(g_0) = e^{-l} \rho_s[g(l)]. \tag{C18}$$

We shall evaluate this relation by following the  $T=0$  trajectory in the Néel phase in Fig. 2(b) down the  $\bar{g} = g/g_c$  axis until  $g(l) \rightarrow 0$  as  $l \rightarrow \infty$ . In this limit [analogous to the  $S \rightarrow \infty$  limit in the microscopic model defined by (1.1)], nonlinear corrections vanish and we can replace  $\rho_s[g(l)]$  on the right-hand side of (C18) by its bare value,  $\rho_s[g(l)] \approx \rho_s^0(l) = [\hbar c/g(l)]\Lambda$ . In this way we derive Eq. (3.8b),

$$\begin{aligned}
\rho_s(g_0) &= \lim_{l \rightarrow \infty} e^{-l} \rho_s[g(l)] \\
&= \hbar c \Lambda \lim_{l \rightarrow \infty} [e^{-l}/g(l)] \\
&= \rho_s^0 \left[ 1 - \frac{g_0}{4\pi} \right],
\end{aligned} \tag{C19}$$

where we have used the solution of Eq. (C16), namely,

$$g(l) = \frac{g_0 e^{-l}}{1 - \frac{g_0}{4\pi}(1 - e^{-l})}. \quad (\text{C20})$$

Equation (3.9) follows from dividing both sides of Eq. (C19) by  $c^2$ . Thus, according to the one-loop approximation, the long-wavelength spin-stiffness  $\rho_s$  and the perpendicular susceptibility  $\chi_\perp$  at  $T=0$  can be written in terms of their bare values as

$$\rho_s = \rho_s^0 \left[ 1 - \frac{\hbar\Lambda}{4\pi\sqrt{\rho_s^0\chi_\perp^0}} \right], \quad (\text{C21})$$

$$\chi_\perp = \chi_\perp^0 \left[ 1 - \frac{\hbar\Lambda}{4\pi\sqrt{\rho_s^0\chi_\perp^0}} \right]. \quad (\text{C22})$$

Note that  $\hbar\Lambda/\sqrt{\rho_s^0\chi_\perp^0} = g_0$ , and that both  $\rho_s$  and  $\chi_\perp$  are predicted to vanish at  $g_c$ , although their ratio  $c^2 = \rho_s/\chi_\perp$  remains finite.

#### APPENDIX D: RENORMALIZATION-GROUP ANALYSIS OF THE STATIC PROPERTIES OF THE CLASSICAL LATTICE ROTATOR MODEL

In this appendix, we shall use the renormalization-group approach to discuss the static properties of the classical lattice O(3) rotator model (also called the nonlinear  $\sigma$  model) in two dimensions. We shall derive an explicit expression for the static structure factor using the one-loop approximation,<sup>22</sup> but many of the results will also be correct more generally in the asymptotic low-temperature limit, as will be indicated at the end. We shall work with the classical limit of Eqs. (3.1), and use in particular the limit of Eq. (3.1b) as  $g \rightarrow 0$  in  $d=2$ ,

$$\frac{dt}{dl} = \frac{1}{2\pi} t^2, \quad (\text{D1})$$

with solution ( $t_0 = k_B T / \rho_s^0$ )

$$t(l) = \frac{t_0}{1 - (t_0/2\pi)l}. \quad (\text{D2})$$

The correlation length, measured in units of the lattice constant  $b$ , obeys

$$\xi(t_0) = e^l \xi[t(l)], \quad (\text{D3})$$

and we choose  $l = l^*$  such that  $t(l^*) = 2\pi$  insuring that we are well out of the critical region  $t_0 \geq 0$ . Assuming for simplicity that  $\xi(t = 2\pi) = 1$ , we find the standard result

$$\xi(t_0) = e^{(2\pi/t_0) - 1}. \quad (\text{D4})$$

We now use a similar matching procedure to calculate

$$S(k, t_0) \equiv b^d \sum_i e^{-i\mathbf{k} \cdot \mathbf{r}_{ij}} \langle \hat{\mathbf{n}}_i \cdot \hat{\mathbf{n}}_j \rangle, \quad (\text{D5})$$

where  $\mathbf{k}$  is measured in units of  $b^{-1}$ . Here, and in the rest of this appendix, we set the parameter  $N_0 = 1$  in Eq. (4.3). It is straightforward to generalize Eq. (3.13) of

and Pelcovits<sup>22</sup> to finite  $k$  and find

$$S(k, t_0) = \exp \left[ 2l - \int_0^l \eta(l') dl' \right] S[e^l k, t(l)], \quad (\text{D6a})$$

with

$$\eta(l) = \frac{n-1}{2\pi} t(l). \quad (\text{D6b})$$

Upon using (D2) and integrating the exponential with  $n=3$ , we find

$$S(k, t_0) = e^{2l} \left[ 1 - \frac{t_0 l}{2\pi} \right]^2 S[e^l k, t(l)]. \quad (\text{D7})$$

We evaluate the static structure factor on the right-hand side of (D7) at  $l = l^*$  to insure that the correlation sum in Eq. (D5) becomes nonsingular either because  $\xi(l) = e^{-l} \xi(t_0) = O(1)$  or because of a sufficiently large rescaled wave vector  $k(l) = k e^l$ . These requirements are satisfied by choosing  $l = l^*$  such that

$$\xi^{-2}(t_0) e^{2l^*} + k^2 e^{2l^*} = 1. \quad (\text{D8})$$

When (D8) is satisfied, we can approximate  $S[e^{l^*} k, t(l^*)]$  by

$$S[e^{l^*} k, t(l^*)] \approx \frac{t(l^*)}{\xi^{-2}(l^*) + k^2(l^*)}, \quad (\text{D9})$$

which has the Ornstein-Zernicke form when  $t(l^*) = O(1)$ , and which gives the correct behavior  $S[k(l^*), t(l^*)] \approx t(l^*)/k^2(l^*)$  as  $t(l^*) \rightarrow 0$  for fixed  $k(l^*)$ . Upon substituting (D9) in (D7) using (D2), we find

$$S(k, t_0) = \frac{t_0 e^{2l^*} [1 - (t_0 l^*/2\pi)]}{\xi^{-2}(l^*) + k^2(l^*)}. \quad (\text{D10})$$

When Eq. (D8) is solved for  $l^*$ , we can use (D4) to put (D10) into a scaling form, namely

$$S(k, t_0) \approx \frac{t_0^2 \xi^2}{2\pi} f(k\xi), \quad (\text{D11})$$

where

$$f(x) = \frac{1 + \frac{1}{2} \ln(1+x^2)}{1+x^2}. \quad (\text{D12})$$

Different choices of matching conditions than (D8) would give rise to slightly different scaling functions, although all reasonable choices will have  $f(x) \propto \ln x/x^2$  for large  $x$ , as in Eq. (4.10). The qualitative behavior of  $S(k, t_0)$  as a function of temperature is sketched in Fig. 5. For fixed  $k$  (the deviation from the antiferromagnetic wave vector in a neutron scattering experiment), one initially has  $S(k, t_0) \sim e^{4\pi/t_0}$  with decreasing  $t_0$ , but eventually  $S(k, t_0)$  rolls over and tends to zero like  $S(k, t_0) \approx t_0/k^2$ . [In a quantum system,  $S(k, t_0)$  approaches a finite constant at  $t_0=0$ , reflecting the zero-point fluctuations.] The maximum in  $S(k, t_0)$  occurs when  $k\xi \approx 1$ , i.e., at

$$t_0^{\max} \approx \frac{2\pi}{\ln(1/k)} \quad (\text{D13})$$

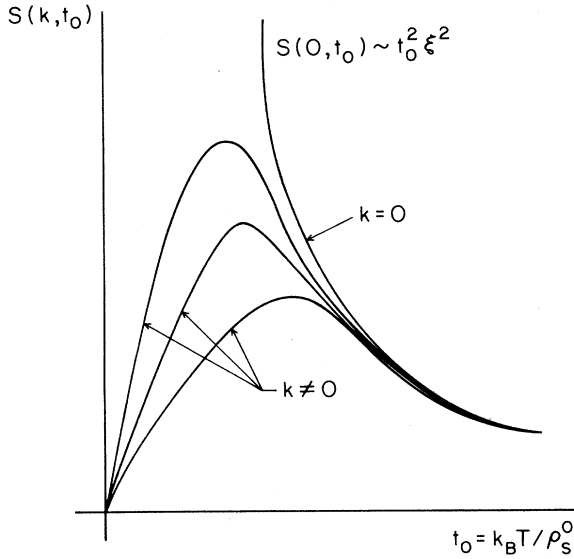


FIG. 5. The qualitative behavior of  $S(k, t_0)$  as a function of temperature for classical lattice rotator model.

and

$$S(k, t_0^{\max}) \approx \frac{2\pi}{\ln(1/k)k^2}. \quad (\text{D14})$$

We can determine the wave-vector-dependent spin stiffness  $\rho_s(k, t_0)$  needed to implement the dynamic scaling hypothesis in a very similar way. The renormalization-group homogeneity relation for the spin stiffness, in  $d$  dimensions, is quite generally<sup>62</sup>

$$\rho_s(k, t_0) = e^{(2-d)l} \rho_s[e^l k, t(l)]. \quad (\text{D15})$$

When  $k \approx \xi^{-1}$  and  $d=2$ , we can use the  $l^*$  defined by Eq. (D8) and approximate the right-hand side of (D14) by  $k_B T / t(l^*)$ . If we use Eqs. (D2) and (D4) we find within one-loop approximation,

$$\rho_s(k, t_0) \approx \frac{k_B T}{2\pi} g(k\xi), \quad (\text{D16a})$$

$$g(x) = [1 + \frac{1}{2} \ln(1+x^2)]. \quad (\text{D16b})$$

In a similar manner, we can discuss the quantity  $N(k, t_0) \equiv \langle |n_{\lambda=k^{-1}}| \rangle$  where  $n_{\lambda}(\mathbf{r})$  is the order parameter at some instant of time averaged over a region of diameter  $\lambda$  centered at point  $\mathbf{r}$ , as discussed in Sec. IV. Scaling relation for  $N(k, t_0)$  can be extracted from Eqs. (2.12) and (2.13) of Ref. 22, and for O( $n$ ) models is found to be

$$\begin{aligned} N(k, t_0) &= \exp \left[ -\frac{n-1}{2\pi} \int_0^l t(l') dl' \right] N[e^l k, t(l)] \\ &= \left[ 1 - \frac{t_0}{2\pi} l \right]^{n-1/2} N[e^l k, t(l)]. \end{aligned} \quad (\text{D17})$$

When  $l^*$  is given by (D8), with  $k = \xi^{-1}$ ,  $N[e^{l^*} k, t(l^*)]$  is of order unity and we have using (D4)

$$N(k = \xi^{-1}, t_0) \sim t_0^{(n-1)/2}. \quad (\text{D18})$$

Finally, we derive an analogous scaling relation for the

deviation of the perpendicular susceptibility  $\chi_{\perp}$  from its isotropic value. From Eq. (4.1) we have

$$\chi_{\alpha\beta} = \frac{2}{3} \delta_{\alpha\beta} \chi_{\perp}^0 + \delta\chi_{\alpha\beta}, \quad (\text{D19})$$

where

$$\delta\chi_{\alpha\beta} = \frac{1}{3} \delta_{\alpha\beta} - \langle \Omega_{i\alpha} \Omega_{j\beta} \rangle \quad (\text{D20})$$

is the traceless deviation of the uniform susceptibility from isotropy. It is sufficient to study  $\delta\chi_{zz}(k, t_0)$ , since  $\delta\chi_{xx} = \delta\chi_{yy} = -\frac{1}{2} \delta\chi_{zz}$ . The scaling behavior of perturbations like  $\delta\chi_{zz}$  was also determined in Ref. 22. Using Eqs. (3.5) and (3.6) of this reference, we find that (for general  $n$ )

$$\begin{aligned} \delta\chi_{zz}(k, t_0) &= \exp \left[ \frac{-n}{2\pi} \int_0^l t(l') dl' \right] \delta\chi_{zz}[e^l k, t(l)] \\ &= \left[ 1 - \frac{t_0}{2\pi} l \right]^n \delta\chi_{zz}[e^l k, t(l)]. \end{aligned} \quad (\text{D21})$$

Upon evaluating this expression at  $l=l^*$ , for  $t_0 \rightarrow 0$  at any fixed value of the product  $k\xi$ , we find

$$\delta\chi_{zz}(k, t_0) \propto t_0^3. \quad (\text{D22})$$

Thus for  $n=3$ , for fixed finite  $k\xi$ , we find

$$\chi_{\alpha\beta} = \frac{2}{3} \delta_{\alpha\beta} \chi_{\perp}^0 [1 + O(t_0^3)]. \quad (\text{D23})$$

Note that (D18) and (D22) can be combined to give the general relation

$$\delta\chi_{zz}(k, t_0) \propto N(k, t_0)^{2n/(n-1)}. \quad (\text{D24})$$

For the quantum antiferromagnet, the short wavelength behavior of  $\chi_{\alpha\beta}(k)$  is obtained more accurately if one writes  $l = \ln(k_B T / \hbar c k)$  and replaces the sharp cutoff of the integral in (D21) at  $l'=0$  by a soft cutoff, provided by the spin-wave Bose occupation factor, as in Sec. V. One then finds that for  $k > \xi^{-1}$ ,

$$\frac{\chi_{\perp}(k, T)}{\chi_{\perp}^0} \approx \frac{2}{3} + \frac{1}{3} \left[ 1 + \frac{k_B T}{2\pi\rho_s} \ln(1 - e^{-\hbar c k / k_B T}) \right]^3. \quad (\text{D25})$$

This ratio increases monotonically from  $\frac{2}{3}$  to 1, as  $k \rightarrow \infty$ . The ratio lies between  $\frac{2}{3}$  and  $\frac{5}{6}$  provided that

$$\frac{\hbar c k}{k_B T} \leq \left[ \frac{\xi}{a} \right]^{0.21}. \quad (\text{D26})$$

Finally, we note that the procedures used in this appendix can be readily generalized to include corrections of two-loop order and beyond. Although the preexponential factor in the expression for the correlation length is modified by the two-loop correction, and the functional form of the dependence of  $S(k, t_0)$  on the parameter  $k\xi$  is not precisely given by Eq. (D12), Eq. (D11) which relates the temperature dependence of  $S(k, t_0)$  to the temperature dependence of  $\xi$  is valid in the limit  $t_0 \rightarrow 0$  for any fixed value of the product  $k\xi$ . Similarly Eq. (D16a) gives the correct form of  $\rho_s(k, t_0)$  in the limit  $t_0 \rightarrow 0$ , and Eq. (D16b) is correct for  $k\xi$  large, but Eq. (D16b) is only approximately correct for  $k\xi$  of order unity. Equations (D18), (D23), and (D24) also remain valid, to leading order in  $t_0$ , for  $t_0 \rightarrow 0$ , when corrections to the one-loop equations are included.

APPENDIX E: DERIVATION OF EQUATIONS  
(5.1) AND (5.2)

In this appendix we show that given our  $O(n)$  invariant QNL $\sigma$ M at any finite temperature  $t \neq 0$ , we can integrate out all quantum fluctuations to obtain an effective  $O(n)$  invariant classical NL $\sigma$ M. The resulting classical problem is defined by Eqs. (5.1) and (5.2). For our purpose it will be sufficient to demonstrate this mapping to one-loop order.

The calculation described below follows along the same line as those given in Appendix C. This time we break up the  $\pi$  field as

$$\pi(\omega_n, q) \equiv \begin{cases} \pi_<(q), & \omega_n = 0, \\ \pi_>(\omega_n, q), & \omega_n \neq 0. \end{cases} \quad (E1)$$

If we can integrate out  $\pi_>(\omega_n, q)$ , we would have a theory involving only  $\pi_<(q)$ , which no longer contains any quantum fluctuations signified by the nonzero Matsubara frequencies. Note that in contrast to Appendix C, we do not break up the  $q$  space into shells. Thus,  $\pi_<(q)$  contains all wave vectors  $q$ . (As in Appendix C, we define  $q$  to be di-

mensionless, and confined to the range  $0 \leq q < 1$ .) Integration of  $\pi_>(\omega_n, q)$  is carried out in one-loop approximation and yields [cf. Eqs. (C9) and (C10)]

$$\left(\frac{u}{g_0}\right)' = \zeta_{th}^2 \left(\frac{u}{g_0} + I_{th}\right), \quad (E2)$$

$$(hu)' = \zeta_{th}^2 [hu + \frac{1}{2} hg_0(n-1)I_{th}]. \quad (E3)$$

The calculation is identical to that in Appendix C. Here

$$I_{th} = \sum_{n \neq 0} \int \frac{d^d k}{(2\pi)^d} \frac{1}{k^2 + \omega_n^2 + hg_0}. \quad (E4)$$

The spin rescaling factor  $\zeta_{th}$  is given by

$$\zeta_{th} = 1 - \frac{1}{2}(n-1)(g_0/u)I_{th}. \quad (E5)$$

The remaining notations are the same as that given in Appendix C. At first sight the appearance of spin rescaling factor  $\zeta_{th}$  may seem unnatural. One should, however, note that by integrating out all quantum fluctuations we have reduced the value of the magnetization.  $\zeta_{th}$  is nothing but the reduction factor. To see this more explicitly let us calculate  $\langle \sigma \rangle$  to one-loop order:

$$\begin{aligned} \langle \sigma \rangle &= \langle \sqrt{1 - \pi^2(x, \tau)} \rangle \approx 1 - \frac{1}{2} \sum_{k, m} \langle \pi^2(k, \omega_m) \rangle = 1 - \frac{g_0}{u} \left(\frac{n-1}{2}\right) \sum_m \int \frac{d^d k}{(2\pi)^d} \frac{1}{k^2 + \omega_m^2 + hg_0} \\ &= 1 - \frac{g_0}{2u}(n-1)I_{th} = \frac{g_0}{2u}(n-1) \int \frac{d^d k}{(2\pi)^d} \frac{1}{k^2 + hg_0} \\ &\approx \left[1 - \frac{g_0}{2u}(n-1)I_{th}\right] \left[1 - \frac{g_0}{2u}(n-1) \int \frac{d^d k}{(2\pi)^d} \frac{1}{k^2 + hg_0}\right]. \quad (E6) \end{aligned}$$

The last line in Eq. (E6) is correct to one-loop order, which is what we are considering here.

Combining Eqs. (E2) and (E5), and Eqs. (E3) and (E5) we get, respectively,

$$\left(\frac{u}{g_0}\right)' = \frac{u}{g_0} - (n-2)I_{th}, \quad (E7)$$

and

$$(hu)' = hu \left[1 - \frac{g_0}{2u}(n-1)I_{th}\right]. \quad (E8)$$

We are now going to concentrate on the problem in two spatial dimensions. For  $I_{th}$  one obtains

$$\begin{aligned} I_{th} &= \frac{u}{2\pi} \int_0^1 dk \frac{k}{\sqrt{k^2 + hg_0}} \\ &+ \frac{1}{2\pi} \ln \left[ \frac{1 - \exp\{-[u\sqrt{hg_0} + (u/\sqrt{hg_0})]\}}{1 - \exp(-u\sqrt{hg_0})} \right] \\ &- \frac{1}{2\pi} \ln \left[ \frac{1 + hg_0}{hg_0} \right]^{1/2}. \quad (E9) \end{aligned}$$

In the limit that the magnetic field (infrared regulator in this case) goes to zero, we get

$$\left(\frac{u}{g_0}\right)' = \frac{1}{k_B T} \left[ \rho_s(0) + \frac{(n-2)k_B T}{2\pi} \ln \left[ \frac{\Lambda \hbar c}{k_B T} \right] \right]. \quad (E10)$$

To one-loop order we, therefore, have Eqs. (5.1) and (5.2). Here  $\rho_s(0)$  is the one-loop renormalization of the spin stiffness at  $T=0$  due to quantum fluctuations [cf. Eq. (C21)]. Explicitly, as in Eq. (C21), we get

$$\rho_s(0) = \rho_s^0 \left[ 1 - (n-2) \frac{\hbar c \Lambda}{4\pi \rho_s^0} \right]. \quad (E11)$$

For  $n=3$ , we get the same result as that in Eq. (C21).

APPENDIX F: MEAN-FIELD MODEL OF  
INTERPLANAR COUPLINGS AT  $T=0$

In this appendix we show how to solve a generalization of the quantum nonlinear  $\sigma$  model (2.3) in which an infinite number of  $2d$  planes are coupled together with nearest-neighbor interplanar coupling  $J'$ . A discretized version of the model will be solved at  $T=0$  in the mean-field approximation. In general, corrections to the mean-field results will be small, because the equivalent classical system is three dimensional when  $J'=0$  and four dimensional when  $J' \neq 0$ . We shall see that, unless the couplings are adjusted to place  $g$  very close to  $g_c$ , there will be negligible corrections to the staggered magnetization of an isolated  $2d$  layer for  $0 < J'/J \ll 1$ .

Our starting point is a stack of  $2d$  quantum antiferromagnets, each described by an effective action like Eq. (2.3) with  $\beta \rightarrow \infty$ . If  $\hat{\Omega}_i(\mathbf{y}, u)$  is the order parameter of

the  $l$ th layer, the total effective action is

$$S_{\text{eff}}/\hbar = \sum_l \int_0^\infty du \int d^d y \left[ \frac{1}{2g_0} \left( |\nabla \hat{\mathbf{n}}_l(u, \mathbf{y})|^2 + \left| \frac{\partial \hat{\mathbf{n}}_l(u, \mathbf{y})}{\partial u} \right|^2 \right) + J' \hat{\mathbf{n}}_l(u, \mathbf{y}) \cdot \hat{\mathbf{n}}_{l+1}(u, \mathbf{y}) \right]. \quad (\text{F1})$$

We regularize (F1) by replacing the continuous variables  $(u, \mathbf{y})$  by a  $(1+2)$  dimensional cubic lattice of sites  $\{\mathbf{r}_i\}$  with lattice constant  $b$ . The resulting model is, up to an unimportant constant,

$$S_{\text{eff}}/\hbar = \frac{b^3}{g_0} \sum_l \sum_{\langle i, j \rangle} \hat{\mathbf{n}}_l(\mathbf{r}_i) \cdot \hat{\mathbf{n}}_l(\mathbf{r}_j) + J' \sum_n \sum_i \hat{\mathbf{n}}_l(\mathbf{r}_i) \cdot \hat{\mathbf{n}}_{l+1}(\mathbf{r}_i). \quad (\text{F2})$$

The mean-field approximation amounts to the replacement

$$S_{\text{eff}}/\hbar \rightarrow \frac{b^3}{g_0} \sum_l \sum_i \hat{\mathbf{n}}_l(\mathbf{r}_i) \cdot \mathbf{h}_l(\mathbf{r}_i), \quad (\text{F3})$$

where the local field is

$$\begin{aligned} \mathbf{h}_l(\mathbf{r}_i) &= [6 + 2g_0 J' b^{-3}] \langle \hat{\mathbf{n}}_l(\mathbf{r}_i) \rangle \\ &\equiv [6 + 2g_0 J' b^{-3}] \mathbf{N}. \end{aligned} \quad (\text{F4})$$

The self-consistent equation for the staggered magnetiza-

tion is readily found to be

$$N = \coth \left[ \frac{6b^3}{g_0} \left( 1 + \frac{g_0}{3} J' b^{-3} \right) N \right] - \frac{g_0}{6b^3 [1 + (g_0/3) J' b^{-3}] N}. \quad (\text{F5})$$

If  $N_0(g_0)$  is the solution of this equation when  $J'=0$ , the solution for  $J' \neq 0$  is

$$\begin{aligned} N &= N_0 \left[ g_0 / \left( 1 + \frac{g_0}{3} J' b^{-3} \right) \right] \\ &\approx N_0(g_0) - \frac{g_0^2 J' b^{-3}}{3} \frac{dN_0(g_0)}{dg_0} \Big|_{J'=0}. \end{aligned} \quad (\text{F6})$$

The derivative  $dN_0/dg_0$  only becomes large very close to the three-dimensional critical point. Away from this singularity the corrections to  $N_0(g_0)$  will be of order  $J'/J$  times a constant of order unity.

\*Permanent address: Department of Physics, University of California at Los Angeles, Los Angeles, CA 90024.

<sup>1</sup>P. W. Anderson, *Science* **235**, 1196 (1987).

<sup>2</sup>See, for example, G. Baskaran, Z. Zou, and P. W. Anderson, *Solid State Commun.* **63**, 973 (1987); P. W. Anderson, G. Baskaran, Z. Zou, and T. Hsu, *Phys. Rev. Lett.* **58**, 2790 (1987); V. J. Emery, *ibid.* **58**, 2794 (1987); J. E. Hirsch, *ibid.* **59**, 228 (1987); S. A. Kivelson, D. S. Rokhsar, and J. P. Sethna, *Phys. Rev. B* **35**, 8865 (1987); C. Gros, R. Joynt, and T. M. Rice, *Z. Phys. B* **68**, 425 (1987); J. R. Schrieffer, X.-G. Wen, and S.-C. Zhang, *Phys. Rev. Lett.* **60**, 944 (1988); A. Aharony, R. J. Birgeneau, A. Coniglio, M. A. Kastner, and H. G. Stanley, *ibid.* **60**, 1330 (1988).

<sup>3</sup>G. Shirane, Y. Endoh, R. J. Birgeneau, M. A. Kastner, Y. Hidaka, M. Oda, M. Suzuki, and T. Murakami, *Phys. Rev. Lett.* **59**, 1613 (1987).

<sup>4</sup>Y. Endoh, K. Yamada, R. J. Birgeneau, D. R. Gabbe, H. P. Jenssen, M. A. Kastner, C. J. Peters, P. J. Picone, T. R. Thurston, J. M. Tranquada, G. Shirane, Y. Hidaka, M. Oda, Y. Enomoto, M. Suzuki, and T. Murakami, *Phys. Rev. B* **37**, 7443 (1988).

<sup>5</sup>S. Chakravarty, B. I. Halperin, and D. R. Nelson, *Phys. Rev. Lett.* **60**, 1057 (1988).

<sup>6</sup>This estimate, which is given in Ref. 5, is in agreement with T. Thio, T. R. Thurston, N. W. Preyer, M. A. Kastner, H. P. Jenssen, D. R. Gabbe, C. Y. Chen, R. J. Birgeneau, and A. Aharony, *Phys. Rev. B* **38**, 905 (1988).

<sup>7</sup>C. J. Peters, R. J. Birgeneau, M. A. Kastner, H. Yoshizawa, Y. Endoh, J. Tranquada, G. Shirane, Y. Hidaka, M. Oda, M. Suzuki, and T. Murakami, *Phys. Rev. B* **37**, 9761 (1988).

<sup>8</sup>P. W. Anderson, *Phys. Rev.* **86**, 694 (1952).

<sup>9</sup>(a) J. D. Reger and A. P. Young, *Phys. Rev. B* **37**, 5978 (1988); (b) D. A. Huse, *ibid.* **37**, 2380 (1988); (c) D. A. Huse and V. Elser, *Phys. Rev. Lett.* **60**, 2531 (1988); (d) R. Shan-

kar and G. Murthy (unpublished); (e) M. Gross, E. Sánchez-Velasco, and E. Siggia (unpublished); (f) S. Liang, B. Doucot, and P. W. Anderson, *Phys. Rev. Lett.* **61**, 365 (1988).

<sup>10</sup>P. W. Anderson, *Mater. Res. Bull.* **8**, 153 (1973); P. Fazekas and P. W. Anderson, *Philos. Mag.* **30**, 432 (1974).

<sup>11</sup>E. J. Neves and J. F. Peres, *Phys. Lett.* **114A**, 331 (1986).

<sup>12</sup>F. J. Dyson, E. H. Lieb, and B. Simon, *J. Stat. Phys.* **18**, 335 (1978).

<sup>13</sup>I. Affleck, T. Kennedy, E. H. Lieb, and H. Tasaki, *Commun. Math. Phys.* **115**, 477 (1988).

<sup>14</sup>P. C. Hohenberg, *Phys. Rev.* **158**, 383 (1967); N. D. Mermin and H. Wagner, *Phys. Rev. Lett.* **17**, 1133 (1966).

<sup>15</sup>C. Kittel, *Quantum Theory of Solids* (Wiley, New York, 1963).

<sup>16</sup>T. Oguchi, *Phys. Rev.* **117**, 117 (1960).

<sup>17</sup>R. B. Stinchcombe, *J. Phys. C* **4**, L79 (1971).

<sup>18</sup>See, however, P. Chandra and B. Doucot, *Phys. Rev. B* **38**, 9335 (1988); M. Inui, S. Doniach, and M. Gabay, *ibid.* **38**, 6631 (1988); S. Doniach, M. Inui, V. Kalmeyer, and M. Gabay, *Europhys. Lett.* **6**, 663 (1988).

<sup>19</sup>For a general discussion of classical nonlinear  $\sigma$  model, see D. J. Amit, *Field Theory, the Renormalization Group, and Critical Phenomena*, 2nd ed. (World Scientific, Singapore, 1984), pp. 364–381.

<sup>20</sup>J. A. Hertz, *Phys. Rev. B* **14**, 1165 (1976).

<sup>21</sup>A. P. Young, *J. Phys. C* **8**, L309 (1975).

<sup>22</sup>D. R. Nelson and R. A. Pelcovits, *Phys. Rev. B* **16**, 2191 (1977).

<sup>23</sup>F. D. M. Haldane, *Phys. Lett.* **93A**, 464 (1983); *Phys. Rev. Lett.* **50**, 1153 (1983).

<sup>24</sup>I. Affleck, *Nucl. Phys.* **B257**, 397 (1985).

<sup>25</sup>See F. D. M. Haldane, in Ref. 23; and I. Affleck, in Ref. 24.

<sup>26</sup>See F. D. M. Haldane, in Ref. 23; *J. Appl. Phys.* **57**, 3359 (1985).

- <sup>27</sup>R. Botet, R. Jullien, and M. Kolb, *Phys. Rev. B* **28**, 3914 (1983); H. J. Blöte and M. P. Nightingale, *ibid.* **33**, 659 (1986).
- <sup>28</sup>E. Lieb, T. Schultz, and D. Mattis, *Ann. Phys. (N.Y.)* **16**, 407 (1961).
- <sup>29</sup>I. Affleck, *Phys. Rev. B* **37**, 5186 (1988). See also the discussion by P. W. Anderson, S. John, G. Baskaran, B. Doucot, and S.-D. Liang (unpublished).
- <sup>30</sup>Z. Zou, *Phys. Lett. A* (to be published).
- <sup>31</sup>I. E. Dzyaloshinskii, A. M. Polyakov, and P. B. Wiegmann, *Phys. Lett. A* **127**, 112 (1988); P. B. Wiegmann, *Phys. Rev. Lett.* **60**, 821 (1988); A. M. Polyakov, *Mod. Phys. Lett. A* **3**, 325 (1988).
- <sup>32</sup>F. Wilczek and A. Zee, *Phys. Rev. Lett.* **51**, 2250 (1983).
- <sup>33</sup>T. Dombre and N. Read, *Phys. Rev. B* **38**, 7181 (1988); E. Fradkin and M. Stone *ibid.* **38**, 7215 (1988); L. B. Ioffe and A. I. Larkin, *Int. J. Mod. Phys. B* **2**, 203 (1988); X.-G. Wen and A. Zee, *Phys. Rev. Lett.* **61**, 1025 (1988); F. D. M. Haldane *ibid.* **61**, 1029 (1988).
- <sup>34</sup>See F. D. M. Haldane, in Ref. 33.
- <sup>35</sup>N. Read and S. Sachdev (unpublished).
- <sup>36</sup>B. D. Josephson, *Phys. Lett.* **21**, 608 (1966).
- <sup>37</sup>K. B. Lyons, P. A. Fleury, J. P. Remeika, A. S. Cooper, and T. J. Negran, *Phys. Rev. B* **37**, 2353 (1988).
- <sup>38</sup>R. J. Birgeneau, D. R. Gabbe, H. P. Jenssen, M. A. Kastner, P. J. Picone, T. R. Thurston, G. Shirane, Y. Endoh, M. Sato, K. Yamada, Y. Hidaka, M. Oda, Y. Enomoto, M. Suzuki, and T. Murakami, *Phys. Rev. B* **38**, 6636 (1988).
- <sup>39</sup>B. I. Halperin and P. C. Hohenberg, *Phys. Rev.* **177**, 952 (1969).
- <sup>40</sup>D. P. Arovas and A. Auerbach, *Phys. Rev. B* **38**, 316 (1988); A. Auerbach and D. P. Arovas, *Phys. Rev. Lett.* **61**, 617 (1988); D. R. Grempel, *ibid.* **61**, 1041 (1988).
- <sup>41</sup>R. P. Feynman and A. P. Hibbs, *Quantum Mechanics of Path Integrals* (McGraw-Hill, New York, 1965).
- <sup>42</sup>B. I. Halperin and P. C. Hohenberg, *Phys. Rev.* **188**, 898 (1969).
- <sup>43</sup>T. Holstein and H. Primakoff, *Phys. Rev.* **58**, 1098 (1940).
- <sup>44</sup>The tensor  $\chi_{\alpha\beta}$  may be identified with the paramagnetic susceptibility tensor in units where the gyromagnetic ratio ( $g\mu_B/\hbar$ ) has value unity. The true magnetic susceptibility for the quantum lattice rotator model in these units should include in addition to the paramagnetic term, a diamagnetic term which is equal to minus the right-hand side of Eq. (4.1). Equation (4.1) is thus a restatement of the well-known theorem that the magnetic susceptibility is zero for a system described by classical mechanics. In the case of Heisenberg antiferromagnet, the diamagnetic term is absent. Therefore, we may identify  $(g\mu_B/\hbar)^2\chi_{\alpha\beta}$  with the actual magnetic susceptibility tensor of the two-dimensional spin system.
- <sup>45</sup>A. B. Harris, D. Kumar, B. I. Halperin, and P. C. Hohenberg, *Phys. Rev. B* **3**, 961 (1971).
- <sup>46</sup>B. I. Halperin, P. C. Hohenberg, and E. D. Siggia, *Phys. Rev. B* **13**, 1299 (1976).
- <sup>47</sup>S. H. Shenker and J. Tobochnik, *Phys. Rev. B* **22**, 4462 (1980).
- <sup>48</sup>M. Fukugita and Y. Oyanagi, *Phys. Lett.* **123B**, 71 (1983).
- <sup>49</sup>S. Itoh, Y. Iwasaki, and T. Yoshié, *Nucl. Phys.* **B250**, 312 (1985).
- <sup>50</sup>E. Brézin and J. Zinn-Justin, *Phys. Rev. B* **14**, 3110 (1976).
- <sup>51</sup>M. Creutz, *Quarks, Gluons, and Lattices* (Cambridge Univ. Press, Cambridge, 1983), Chaps. 12 and 13.
- <sup>52</sup>W. Bernreuther and F. J. Wegner, *Phys. Rev. Lett.* **57**, 1383 (1986).
- <sup>53</sup>See, for example, J. Kogut, *Rev. Mod. Phys.* **55**, 775 (1983) (especially pp. 795–800), and references therein.
- <sup>54</sup>G. Parisi, *Phys. Lett.* **92B**, 133 (1980).
- <sup>55</sup>M. E. Lines, *Phys. Rev.* **135**, A1336 (1964).
- <sup>56</sup>E. Manousakis and R. Salvador, *Phys. Rev. Lett.* **60**, 840 (1988).
- <sup>57</sup>D. Vaknin, S. K. Sinha, D. E. Moncton, D. C. Johnston, J. M. Newsam, C. R. Safinya, and H. E. King, Jr., *Phys. Rev. Lett.* **58**, 2802 (1987).
- <sup>58</sup>See, e.g., M. Ma, B. I. Halperin, and P. A. Lee, *Phys. Rev. B* **34**, 3136 (1986); D. Andelman and A. Aharony, *ibid.* **31**, 4305 (1985).
- <sup>59</sup>G. Murthy, *Phys. Rev. B* **38**, 5162 (1988).
- <sup>60</sup>H. Goldstein, *Classical Mechanics* (Addison-Wesley, New York, 1950).
- <sup>61</sup>L. D. Landau and E. M. Lifshitz, *Quantum Mechanics* (Pergamon, New York, 1965), Chap. XI.
- <sup>62</sup>J. Rudnick and D. Jasnow, *Phys. Rev. B* **16**, 2032 (1977).